MODELLING OF POPULATION DYNAMICS IN CELL CULTURES

by

Çiğdem Aksu

B. S., Electrical and Electronics Engineering, Boğaziçi University, 2007

Submitted to the Institute for Graduate Studies in
Science and Engineering in partial fulfillment of
the requirements for the degree of
Master of Science

Graduate Program in Electrical and Electronics Engineering
Boğaziçi University

2010

ACKNOWLEDGEMENTS

First of all, I would like to thank my thesis supervisor Yağmur Denizhan who introduced me to the main subject of my thesis, the population dynamics, which I found very interesting throughout my study. I am grateful to her for the time she devoted to this thesis.

I would like to thank Mehmet Ozansoy for his generosity to share his knowledge on biology with me, and for his help in laboratory during experiments.

I would like to thank members of my thesis jury, Işıl Bozma and Haluk Bingöl for their interest on my work and their valuable time that they spent on reading my thesis.

I owe a word of thanks to my friends in both BUSIM and DSL: Doğan, Sinan, Oya, Kamil, Deniz, Arman. I am grateful to them for their friendship and helps during the different stages of my thesis. With them, the time I spent in office was always filled with many laughters and cheerful conversations, and the problems were solved more easily.

I thank Ersen for his lately helps during the final stages of this thesis. Although initially he was more inclined to distract my attention with *Salinger* and *Morrissey*, I guess he compensated my stolen time.

Finally, I would like to thank my parents and my lovely sister *Meltem*. Without their love and support, this thesis would not be possible like many other things in my life.

ABSTRACT

MODELLING OF POPULATION DYNAMICS IN CELL CULTURES

In this thesis, two models at different resolution levels are developed for the population dynamics of animal cell cultures at the mitotic stage.

The first model is a biologically plausible cellular automata-like micro-model allowing distributed representation of the cell population in a flask, while the second one is a nonlinear type of macro-model based on a lumped representation of the total population and the total toxicity in the flask.

As a specific application C2C12 cell cultures are studied. Experimental data have been gathered from such cultures, and used to tune the parameters of the micro-model. Similarly, the parameters of the macro-model have been tuned to the simulation results obtained from the micro-model.

Comparison of the results show that the proposed micro-model is capable of representing the population dynamics at the mitotic stage with sufficient accuracy while the proposed macro-model can provide a good representation only under the assumptions that the flask is initially clean, and that the initial cell population is sufficiently large and uniformly distributed.

Using experimental data of any cell culture, theoretically it should be possible to tune both models to represent the population dynamics of the respective cell culture.

Another contribution of this theses beside the macro- and micro-models is a software tool which renders the process of cell counting easier and more accurate.

ÖZET

HÜCRE KÜLTÜRLERİNDEKİ NÜFUS DİNAMİĞİNİN MODELLENMESİ

Bu tezde, mitotik evredeki hayvan hücresi kültürlerindeki nüfus dinamiği için farklı çözünürlükte iki model geliştirilmiştir.

İlk model, kaptaki hücre nüfusunun dağıtık gösterimine imkan veren biyolojik açıdan makul, hücresel otomat benzeri bir mikro-model, ikincisi ise kaptaki toplam nüfus ve toplam kirliliği temel alarak topaklanmış bir gösterim sağlayan doğrusal olmayan bir makro-modeldir.

Özellikle C2C12 hücre kültürleri çalışıldı. Bu hücre kültürlerinden toplanan deneysel veri mikro-modelin parametrelerini ayarlamak için, mikro-model simulasyonları sonucu elde edilen veri de makro-modelin parametrelerini ayarlamak için kullanıldı.

Karşılaştırılan sonuçlar, önerilen mikro-modelin mitotik evredeki nüfus dinamiğini yeterli hassasiyetle temsil edebildigini göstermiştir. Ancak önerilen makro-model, kabın başlangıçta temiz olması ve başlangıçtaki nüfusun yeterince kalabalık ve homojen dağılımlı olması koşulları altında iyi bir gösterim sağlamaktadır.

Mitotik evredeki herhangi başka bir hücre kültüründen elde edilen veriler kullanılarak parametreler ayarlandığı takdirde, teorik olarak her iki modelin de bu hücre kültürünün nüfus dinamiğini temsil edebileceği beklenmektedir.

Mikro- ve makro-modellere ek olarak bu tezin başka bir katkısı da hücre sayma işlemini daha kolay ve hassas kılan bir yazılımdır.

TABLE OF CONTENTS

LIST OF FIGURES

LIST OF TABLES

LIST OF SYMBOLS/ABBREVIATIONS

A	amount of nutrition taken by any cell at each time step (micro-model)
D	Diffusion coefficient of toxicity (micro-model)
$\bar{E}(k)$	Average energy at time k (micro-model)
E^{div}	Division energy (micro-model)
E_{min}	Minimum energy of living cells (micro-model)
$E^{rem}(x)$	Amount of energy needed to remediate the damage caused by the local toxicity x on a cell (micro-model)
$E^{rem}_{i,j}(k)$	Amount of energy needed to remediate the damage caused by the local toxicity on any cell at locus (i,j) at time k (micro-model)
$E_{i,j,l}(k)$	Total energy of the l^{th} cell at locus (i,j) at time k (micro-model)
$\underline{F}(\underline{X})$	Non-linear vector function representing the dynamics of a deterministic autonomous system with state vector $\underline{X}$
K	Carrying capacity of an environment in the Verhulst model
k	Discrete time instant (micro-model)
k_{double}	Doubling time of the total population
$m_{i,j}(k)$	Total number of cells located at locus (i,j) at time k (micro-model)
N	Total number of cells in the flask (macro-model)
n	Dimension of the square matrix used to model flask
x	Total toxicity in the flask (macro-model)
$\bar{x}$	Average toxicity in the flask
$x_{i,j}(k)$	Amount of toxicity at locus (i,j) at discrete time instant k (micro-model)
$x(i,j,k)$	Amount of toxicity at discrete space position (i,j) at discrete time instant k (micro-model)
$x(i,j,t)$	Amount of toxicity at continuous space position (i,j) at continuous time instant t (micro-model)

$x^r_{i,j,l}(k)$	Amount of toxicity released by the l^{th} cell at locus (i, j) at time k (micro-model)
$x^r_{i,j}(k)$	Total amount of toxicity released to locus (i, j) at at time k (micro-model)
t	Time
z	Maximum number of cells that a locus can accommodate (micro-model)
α	A parameter in the remediation energy function (micro-model)
β	Ratio of the constant amount of toxicity released by a cell to the constant amount of nutrition taken by a cell per time step (micro-model)
γ	A parameter in the remediation energy function (micro-model)
Δi	Difference between abscissas of two neighboring loci (micro-model)
Δj	Difference between ordinates of two neighboring loci (micro-model)
Δk	Time step in the diffusion process (micro model)

ATP	Adenosine triphosphate
C2C12	Mouse myoblast cells
CA	Cellular automaton
DMEM	Dulbecco's Modified Eagle's Medium
DNA	Deoxyribonucleic acid
ECACC	European Collection of Cell Cultures
FBS	Foetal Bovine Serum
FTCS	Forward-time centered-space
G0	State of quiescence
G1	First growth phase in cell cycle
G2	Second growth phase in cell cycle
M	Mitotic phase in cell cycle
NEAA	Non-Essential Amino Acids

ODE	Ordinary differential equation
PBS	Phosphate-buffered saline
PDE	Partial differential equation
S	Synthesis phase in cell cycle
SIR	Susceptible-infected-resistant

1. INTRODUCTION

Population dynamics is one of the oldest branches of the mathematical biology. As its name suggests, population dynamics studies changes in the size and/or composition of the individual entities in a population, as well as the environmental and biological factors that lead to these changes.

The initial focus of population dynamics was on the area of demography. In other words, population dynamics has first emerged in order to study and analyze the human population. The first breakthrough in population dynamics can be attributed to T. Malthus, who proposed his well-known exponential law for animal populations. In 1798, Malthus claimed that animal populations grow exponentially up to a certain limit, where this limit is mainly determined by the available resources in the habitat of the population [2]. Although, at first sight, this exponential law might seem to be simple to cover the entire complex nature of a population, Malthusian model has found many validations in populations of various species. To name a particular example, the world population is reported to grow exponentially between 1950-1985 [3]. In Malthus' exponential law, the growth rate of the population is chosen to be constant. Later, Malthusian model has been extended to include non-constant growth rates, varying according to the current population size, as suggested by B. Gompertz in 1825 [4] and P. F. Verhulst in 1838 [5]. Especially, Verhulst's model has gained a broad popularity and is commonly known as the *logistic equation*. After Gompetz and Verhulst incorporated the non-constant growth rates into Malthusian model, an important observation along this line has been reported by W. C. Allee [6]. In particular, Allee has observed that the reproduction and survival of individuals decrease in smaller populations and it can lead to the extinction of the population. This phenomenon is commonly known as the *Allee effect*.

While the Malthusian model and its extensions by Gompertz and Verhulst are of interest in population dynamics involving only a single species, V. Volterra's studies on fisheries have advanced the population dynamics to account for interactions between

two different species [7,8]. In particular, V. Volterra has studied the interaction between two species: one of them consisting of predators and the other of preys. Since a similar model was also proposed by A. J. Lotka, now this model is commonly known as the *Lotka-Volterra prey-predator model*. In this prey-predator model, the growth of one population occurs at the expense of the other population directly. In some environments, instead of such a direct link between two populations, there may be a relatively indirect link originating from the share of a common resource like food or water. The corresponding model is known as the *competitive Lotka-Volterra model*, in which there two species competing for the same resource.

In Lotka-Volterra models, the interaction between two different species has been addressed, however, until 1920's the change in the composition of a single population has not been considered. In other words, all of the pr5evious models consider the members of population identical and none of them has studied the interaction between the sub-populations of a single population. This has been addressed by A. G. McKendrick and W. O Kermack, who have proposed the well-known *susceptible-infected-resistant* (SIR) model to study the pattern of spread of epidemics in a population [9]. (This is also why A. G. McKendrick and W. O Kermack's model is called the SIR model.) SIR model considers a population of fixed size, where the entire population is divided into three sub-groups consisting of susceptible, infected, or resistant members, respectively, and studies the demographical interactions between these sub-populations. A. G. McKendrick has also proposed a model [10] accounting for the age distribution in populations somewhat in the same spirit as an earlier model by Sharpe and Lotka [11]. This *Sharp-Lotka-McKendrick model* can be seen as the first example of structured population models, where the term structure refers to the fact that in these models individuals of a population are characterized in terms of personal properties, like age, size, spatial position, that continuously vary over time.

With its achievements in comprehension and analysis of the spreading pattern of epidemics, population dynamics has turned out to be a reliable discipline applicable to almost all branches of biology. To name a few examples, many studies in the fields of pathology, epidemiology, immunology, and genetics have been carried out un-

der the umbrella of population dynamics. In these studies, population dynamics has mostly focused on demographic patterns of cell cultures. *Cell cultures* allow the observation and study of the behavior of cell colonies under controlled conditions, such as the growth process of cells coming from the same tissue in laboratorial set-up where all environmental conditions, such as nutrient, temperature etc., are determined and controlled by scientists. Even without being equipped with the analytical tools of population dynamics, cell cultures provide the biologists with reproducible and consistent demographic results, as well as an extensive framework for the analysis of cell behavior under different conditions.

However, in spite of these advantages provided by cell culture studies there is still a need for advanced analytical tools that can produce reliable estimates of the results of time-consuming cell culture experiments and analyze the huge amount of data obtained from these experiments. At this point, population dynamics provides an analytical framework to (re)produce these experiments within a computational model in a shorter time as well as to analyze the experimental results with the goal of extracting the key factors that determine the growth process of the cell culture of interest. For example, although there has been an intense research activity, both in vivo and in vitro, to understand the main factors determining the growth kinetics and spatial structure of tumors in different growth stages, the lack of population dynamics' analytical models slows down these works despite the extensive experiments carried out.

Using population dynamics, biological populations can be analyzed at various organizational levels, such as cell level, gene level or biomolecular level. Since this thesis focuses is on cell culture populations at cell level, now we provide some background information about population dynamics studies carried out for the analysis of biological populations at cell level. Population models used in these studies can be categorized depending on i) whether the model involves a deterministic or probabilistic set-up, ii) whether the model treats the population as a single macro-sized dynamic system or as a group composed of many interacting sub-systems, iii) whether time is modelled as discrete or continuous, and iv) whether a discrete or continuous space model is used. Below, these categories are explained in further detail:

- Probabilistic Models versus Deterministic Models: In a deterministic model the dynamic behavior of the system variables defined in the model is uniquely determined by the system parameters and the initial conditions of the state variables. In population dynamics, the Malthusian model and its extensions by Gompertz and Verhulst constitute the earliest examples of deterministic models [2, 4, 5]. These early models are quite primitive in the sense that they consider only the size of the population under the effect of the environmental conditions such as the carrying capacity of the environment determined by available resources or space. Representation of the attributes of populations and their environment in terms of fixed parameters can usually be rather restrictive. Instead, other researchers prefer to represent these attributes as random variables which adequate distributions. When one needs to include in the model attributes such as the stage of the cells in their cell cycle [12–16] the composition of different cell types in the culture [17–19], mostly probabilistic models may be preferable. For example, if a model aims to estimate not only the population size of a cell culture but also its composition as a mixture of different cell types, then a probabilistic model may be needed in order to account for the dynamics of conversion from stem cells into different cell types.
- Macro versus Micro Models: A population can be modelled by considering the entire population as a single homogeneous system that can be represented in terms of some lumped macro variables or as a set of spatially distributed and interacting sub-systems, which can consists of different sub-groups or individual cells [2, 5]. The latter type, which will be referred to as micro-models because it accounts for attributes and dynamics at the micro-organizational level, is preferable especially when the population is heterogeneous, i.e. consists of cells with different functionalities. For example, a stem cell culture is composed of various kinds of cells such as mitotically active, quiescent, and differentiated cells, and each of these cell types exhibit different functionalities. Consequently, it does not lend itself to a representation in terms of macro variables which are blind to the local and individual differences of the population members. This is why most population models focusing on heterogeneous cell cultures are based on micro-representations [20–24].

- Discrete versus Continuous Time and Space: Dynamic systems, depending on their nature and the preferred resolution of analysis, have to be put into a framework where the independent variable (time) and the space coordinates are treated either as discrete or continuous variables. While differential equations constitute the most adequate mathematical formalism for continuous-time dynamics [25–28], discrete-time dynamics require description in terms of difference equations [29–31]. On the other hand, partial derivatives are used in the analytical representation of continuous-space systems, whereas discrete-space systems typically ask for numerical simulation. In any case, for purposes of simulation and computer-based analysis both time and space have to be discretized. Discrete-time discrete-space population models have a special importance among all classes of the population models, because even though a population may evolve over continuous time and space, it needs to be discretized for numerical analysis. One of the most commonly used tools employed for the simulation of discrete-time discrete-space dynamics is the formalism called *Cellular Automata* (CA). As the name suggests, the main idea of CA has been borrowed from biology, from the dynamic interactions of neighboring cells in an organism, and been successfully used as a modeling tool in various fields.

A CA is a discrete model defined on a finite-dimensional and limited space consisting of a regular grid of points. Associated with each grid point there exists a set of neighboring grid points and a set of rules regulating the interactions with these neighbors. Each grid point can take on one of the discrete and finite number of possible states at a given time step [31]. The state of a grid point evolves over time according to this point's current state as well as the current states of its neighbors. A CA is a model of local interactions between microscopic entities in a dynamic system, thus it provides a framework for distributed representation of populations. Simulating a CA one can gain an insight into the macroscopic behavior of the entire population.

Although discrete-time discrete-space (micro) models are desirable for the representation and analysis of local interactions, lumped-parameters approximate macro-models describing the total average behavior of an entire population in terms of an

ordinary differential equation may be preferable for purposes of analyzing and predicting the average behavior as well as qualitative evaluation. Tools of nonlinear dynamics can be employed in order to construct and analyze such continuous-time (lumped-parameter) macro-models.

In this thesis, original population dynamics models have been developed at two different levels: a deterministic discrete-time discrete-space micro-model and a deterministic continuous-time continuous-space macro-model. These models are intended to represent the evolution of the population size at the mitotic stage of cell cultures. As an example mouse myoblast cells (C2C12) have been chosen. Because data about the dynamics of population sizes in animal cell cultures are not available in the literature, experimental data gathering has become part of this thesis.

The micro-model is a biologically plausible CA-like model designed in order to account for the population dynamics in cell cultures at their mitotic stage. Unlike most classical CA models it is deterministic and involves also a representation of the environmental dynamics. It should be noted that the term "cell" in Cellular Automata (CA) is used to denote the individual grid points on the discrete space in order to describe interactions between neighboring points with reference to a metaphor of interactions between neighboring cells in an organism. However, in the CA-like micro-model suggested in this thesis the term "cell" is reserved for actual (biological) cells in a cell culture, while the grid points will be referred to as loci (singular: locus). At any given time instance each (biological) cell in this micro-model is characterized by various properties like its energy, its cellular status (mitotically active or quiescent), and age. The environment in this micro-model is represented as a regular grid where each locus contains a constant amount of nutrient and a varying amount of toxicity. The micro-model provides deterministic rules for the interaction between the cells and their environment. This micro-model contains several parameters like amount of nutrition, rate of diffusion of toxicity etc. which have been tuned in order to bring the simulation results obtained from the micro-model into good agreement with the experimental data. Having such a reliable simulator is advantageous, especially one wants to observe the long-term population dynamics of a cell culture, because acquiring experimental

data for the long-term studies is a time-consuming and expensive process. Moreover, the long-run estimates for the population dynamics of a cell culture produced by the proposed CA-like model can be used in the validation of the analytical macro-models proposed for the population dynamics of this cell culture.

The macro-model, is designed in order to approximate the average dynamics of a homogeneously distributed cell population. The form of the differential equation is partially theoretically constructed and partially derived from the simulation results obtained from the micro-model. The macro-model describes the population dynamics on a state space spanned by two state variables: the total population size and the total amount of toxicity in the flask. Once tuned to match the real data, such a macro-model is useful for making theoretical predictions and qualitative evaluations without any need for numerical simulations. However, because practical limitations allow only very scarce experimental data, the strategy adopted in this thesis was to tune the parameters of a biologically plausible micro-model to the experimental data and then to fit a system-theoretically plausible macro-model to the micro-model simulation results.

The relevant biological information about cell cycle dynamics with a special emphasis on the C2C12 cells is given in the second chapter. Experimental setup and methodology used for data gathering from C2C12 cell cultures are explained in the third chapter. In the fourth chapter, both the CA-like micro-model and the analytical macro-model developed for cell cultures are presented. In the fifth chapter, the simulation results obtained from both models are given and compared to experimental data. The sixth and last chapter provides an evaluation of the proposed models and concludes with suggestions for further research.

2. CELLULAR DYNAMICS

Although cells might differ in various ways, all cells still exhibit a similar life cycle. After its initial appearance, every cell grows up until a certain size, where, in general, the size of a cell can be measured by its surface to volume ratio. In other words, a cell grows up to its surface to volume ratio reaches a certain limit (critical ratio), which may be different for different cell types, and even for the same type under different environmental conditions. When the surface to volume ratio of a cell is about to exceed the certain limit for this ratio, cell's membrane cannot gather sufficient supply from its environment for its survival. At this point, to alleviate this danger, the cell undergoes a mitotic division [32], giving birth to two identical daughter cells whit surface to volume ratio less than the critical level. Mitotic division lets the organism keep growing, as well as repairing itself. However, there are some cells like nerve and muscle cells which cannot perform a mitotic division after a certain stage of their life cycle. Initially, these cells also have the mitotic division capability, however after some time, they differentiate into specialized cells and lose their division capability. Despite the absence of mitotic division capability, they can function properly in the organism. Indeed, similar to the specialized cells, other cells also lose their mitotic division capability once they are mature enough. In this chapter, the cell cycle will be explained in detail in addition to the specific properties of C2C12 cells and their cultures.

2.1. Cell Cycle

Every cell has a cell cycle which, roughly, is a sequence of cell growth, DNA replication, and cell division. In particular, the cell cycle is an ordered set of events, culminating in cell growth and division into two daughter cells. The cell cycle consists of four stages which are G1, S, G2 and M stages, designated "GAP 1", "Synthesis", "GAP 2", "mitosis" respectively. The latter corresponds to the stage when nuclear (chromosomes separate) and cytoplasmic division (cytokinesis) occur [33]. Moreover, the G1, S, and G2 stages of a cell between its two consecutive M stages is called

interphase, which, indeed, corresponds to the longest part of a cell cycle. After M

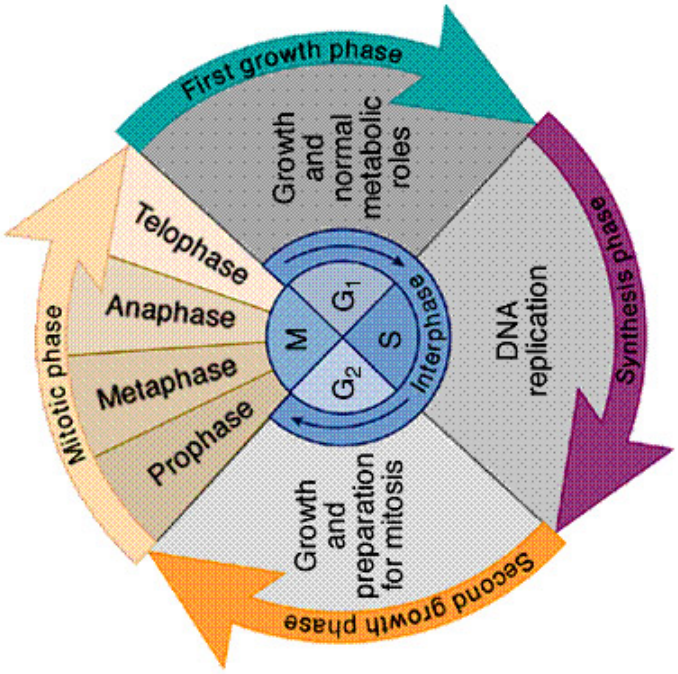

Figure 2.1. The four main phases of the cell cycle [1].

stage, two daughter cells arise as a result of the mitotic division. The daughter cells, after the previous division, are quite small and low on adenosine triphosphate (ATP). ATP is a multifunctional nucleotide used in cells as a coenzyme. It is often called the "molecular unit of currency" of intracellular energy transfer. ATP transports chemical energy within cells for metabolism. It is produced by photophosphorylation and cellular respiration and used by enzymes and structural proteins in many cellular processes, including biosynthetic reactions, motility, and cell division [34]. Cells acquire ATP and increase in size during the G1 phase of interphase. After acquiring sufficient size and ATP, the cells then undergo DNA synthesis. Hence, they harvest ATP which leads them to increase in size during the G1 phase of interphase. After they gather sufficient ATP, and reach to a certain size, their S stage starts, where they synthesize DNA. In particular, they replicate the original DNA molecules yielding two identical copies of the DNA molecule, one for each new cell that will appear after the division. Since the DNA replication is an energy draining process, the cell undergoes a second growth and energy acquisition stage, i.e., the G2 phase starts. The energy saved during G2 is used in mitosis (M phase) [35, Chapter 7].

Mitosis is the process that facilitates the equal partitioning of replicated chromosomes in S phase. It consists of nuclear division and cytokinesis, and produces two identical daughter cells during prophase, metaphase, anaphase, and telophase (Figure 2.2). The detailed information about these phases are as follows [33, 36]:

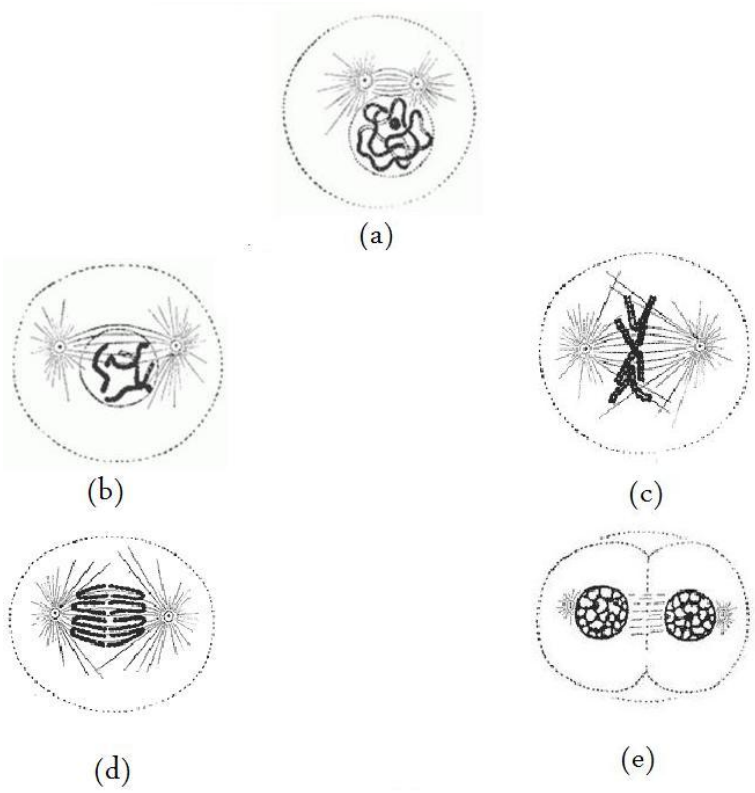

Figure 2.2. Phases of mitosis: (a) Prophase, (b) Prometaphase, (c) Metaphase, (d) Anaphase, (e) Telophase

- During prophase, the replicated chromosomes in the S stage gets highly condense such that chromosomes become very thick and short. However, they are still contained within the nuclear envelope. In the late parts of the prophase, this nuclear envelope breaks down, and within 6 minutes of this breakdown, the mitotic spindle begins to grow with one on each side of the nucleus.
- Prometaphase starts with the dissolve of nuclear membrane. Once the nuclear envelope has broken down, the spindle microtubules and the chromosomes are no longer separated by a membrane boundary. The microtubules begin to interact

with the chromosomes, and the chromosomes undergo what is known as congressional movement toward the center of the spindle. This line is referred to as the metaphase plate. This organization helps to ensure that when the chromosomes are separated, each new nucleus will receive one copy of each chromosome.

- Anaphase commences with the initial splitting of sister chromatids at their centromeres. These daughter chromosomes then begin to separate from each other, each moving away from the metaphase plate and toward one of the two spindle pole regions.
- In telophase, the chromosomes have moved close to the spindle pole regions, and the spindle midzone begins to clear. In this middle region of the spindle, a thin line of vesicles begins to accumulate. The vesicle aggregation event is a harbinger to the assembly of a new cell wall that will be positioned midway along the length of the original cell. It will form the boundary between the newly separating daughter cells.

In animal cells, cytokinesis results when a fiber ring composed of a protein called actin around the center of the cell contracts pinching the cell into two daughter cells, each with one nucleus. Cytokinesis ends the cell division process, and the cycle returns to the beginning of the growth stage G1 for each daughter cell. Time needed for completing a cell cycle differs from cell to cell. However, not all cells complete the entire cell cycle. The cells that have temporarily or reversibly stopped dividing are said to have entered a *state of quiescence* called G0 phase. Lack of growth factor or nutrient and contact inhibition are the primary causes for cells entering G0 phase [37,38]. During the G0 phase, cells perform their main functions except division, and they remain in G0 phase until there is a reason for them to divide, like the increase in the amount of nutrient or diluting population density by subculturing in cell cultures in order to prevent contact inhibition.

Some cell types in mature organisms, such as parenchymal cells of the liver and kidney, enter the G0 phase semi-permanently and can only be induced to begin dividing again under very specific circumstances. Other types of cells, such as epithelial cells, continue to divide throughout an organism's life and rarely enter G0. The nerve cells

and heart muscle cells become quiescent when they reach maturity because they are terminally differentiated. Multi-nucleated muscle cells that we are working on are also often referred to as in the G0 stage.

2.2. C2C12 in Cell Cultures

C2C12 is a mouse myoblast cell line (Figure 2.3). C2C12 cells were originally obtained by Yaffe and Saxel through serial passage of myoblasts cultured from the thigh muscle of C3H mice after a crush injury. These cells are capable of differentiation. C2C12 cells are a useful tool to study the differentiation of myoblast and osteoblast, to express various proteins, and to explore mechanistic pathways [33].

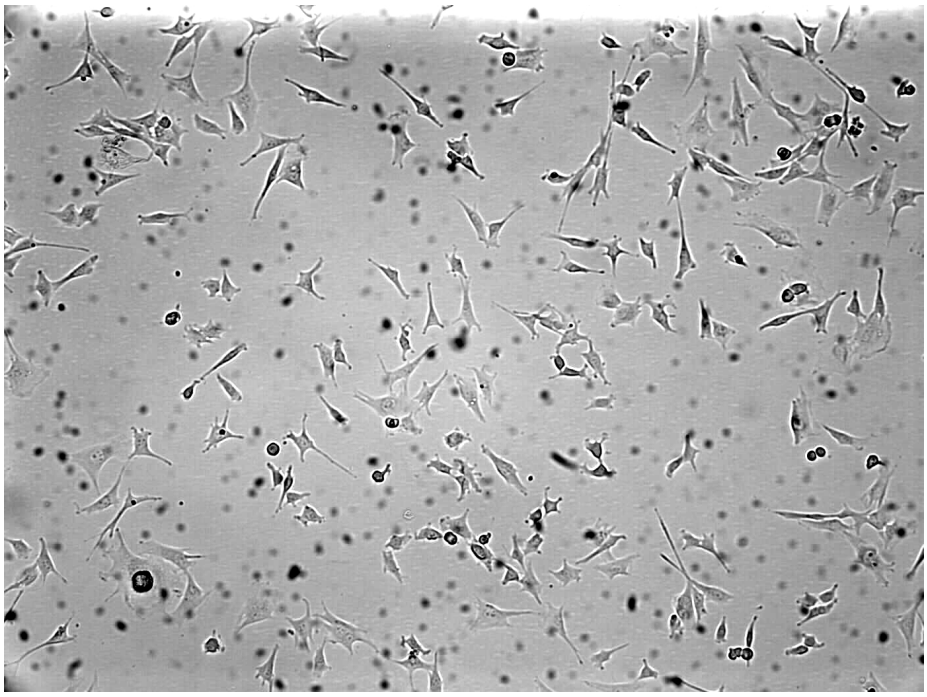

Figure 2.3. The C2C12 cells in cell culture

The C2C12 cell line differentiates rapidly, forming contractile myotubes and producing characteristic muscle proteins. Cultures must not be allowed to become confluent as this will deplete the myoblastic population in the culture. Myotube formation

is enhanced when the medium is supplemented with 10% horse serum instead of fetal bovine serum. However, when myoblasts fills the flask area, they also starts differentiation in small amounts.

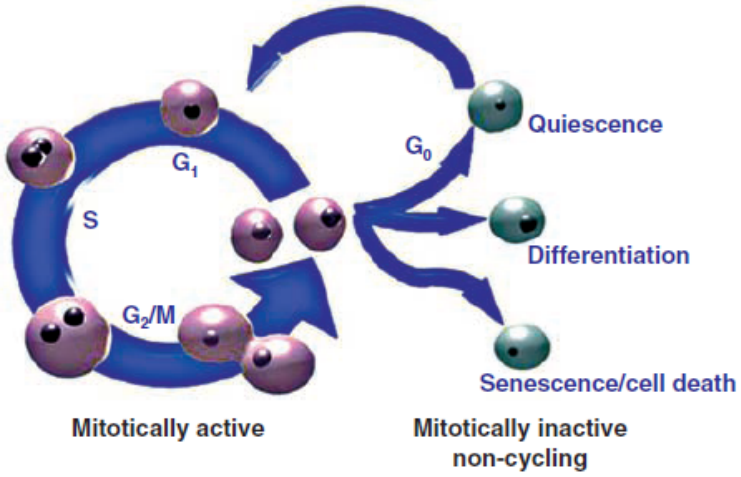

Figure 2.4. The shematic illustration of mitotically active and in-active cell stages

.

In a cell culture, the C2C12 cells can be in one of five stages, biologically recognized as mitosis, quiescence, differentiation, senescence and death (Figure 2.4) [39]. If a cell is mitotically active, its cell cycle consists of growth and division processes. In a cell culture, there is enough nutrient for cells, thus the main reason for a cell going into a mitotically inactive state is the so-called contact inhibition which results from scarcity of the space. If a cell is surrounded by other cells, it cannot divide itself, and becomes quiescent. However, becoming quiescent is reversible, in the sense that if a C2C12 cell is in quiescence state (G0), depending on the environmental conditions, it might become mitotically active again. In our case, this environmental condition is the cell population around the quiescent cell. Thus, if this population decreases, the quiescent cell might be mitotically active again, i.e., continues its cell cycle by dividing itself into two daughter cells. We note that, contrary to the quiescence stage, still there are irreversible states such as differentiation, senescence and death. As mentioned earlier,

C2C12 cells have ability to differentiate themselves to form myotubes. The differentiation occurs when cells fill the flask base. When cells are differentiated, they perform their main metabolic functions except division. Another reason of cells' becoming mitotically inactive is senescence. If a cell becomes older, it loses its division capability, and eventually dies. In cell cultures, since there is sufficient nutrient, and the other conditions affecting the growth are generally good, the primary cause of cell expiration is over-population in the flask. Thus, change in the environment and senescence are rarely observed.

3. Experiment

In this thesis, population size data as a function of time are needed to tune the parameters of the micro-model and compare the results of the micro- and macro-models. Since no such data is available for animal cells, they have been gathered by experiments. In this chapter, the setup and the methods used in these experiments are described.

3.1. Experimental Setup

The C2C12 cell line was purchased from ECACC (European Collection of Cell Cultures) and maintained in its respective growth medium at a density of 2-5x100,000 cells/ml, in a humid 37°C incubator supplied with 5% CO_2. The C2C12 cells were grown in culture flasks in DMEM (Dulbecco's Modified Eagle's Medium) supplemented with penicillin/streptomycin (100 $\frac{\text{units}}{\text{ml}}$ / 100 $\frac{\mu\text{g}}{\text{ml}}$), glutamine (2 mM), 1X NEAA (Non-Essential Amino Acids), and 10% FBS (Foetal Bovine Serum). In order to split the adherent cells, cell monolayers were rinsed with sterile PBS (Phosphate-buffered saline) and trypsinized in 500 μl, 0.05 per cent Trypsin/EDTA for three minutes at 37°C. Following dislocation of cells, trypsin was inhibited with 10 ml complete medium, and the cells were centrifuged at 1500 rpm for five minutes. Cell pellets were resuspended in complete medium and split an desired proportion.

3.2. Methodology

Population data are gathered from cell cultures in two ways traditionally. In the first one, cells are split from the culture by using the method described in section 3.1. A small portion of the split cells are resuspended and divided into three groups. Cells in each small group are counted under the microscope. Next, the average of these three countings is used to estimate the total number of cells in the entire culture. Since cells are removed from the flask, no more data can be obtained from the experiment. Therefore if a sequence of data is needed as in our case, this method is not feasible. In

our case, cells are placed into gridded flasks. The size of the cell population, which is relatively homogeneously distributed on the flask area, is estimated from the population count carried out on a small sample set of grid meshes, rather than a complete count of the entire population.

In first experiment, the population density was selected to be 1/20 which lead to a dilute population. Consequently, the counting process introduced earlier is relatively practical to obtain confident data. However, in the third experiment, the population density was selected to be 1/10 which lead to a highly populated flask. Thus counting cells under the microscope was not practical especially towards the end of experiment when the population becomes rather large. In this case, a Matlab-based software is proposed to count cells.

3.2.1. Cell Counting Software Aid

Because counting cells under the microscope becomes increasingly inefficient as the cell densities increase, photos of the chosen grid meshes were taken in order to

carry out the counting process outside the laboratory under more comfortable conditions. However the quality of the photos do not allow proper identification of the cells (Figure 3.1(a)). Using relatively simple image processing techniques, these photos have been enhanced such that cells can be easily identified (Figure 3.1(b)). This enhancement is achieved by a Matlab-based software (Appendix B) which uses the following algorithm:

- Increasing the intensity range of image from [0.5, 0.75] to [0 1]
- Noise reduction by lowpass Gaussian filtering of size 4

Total cell number is counted automatically by the software and the total cell numbers written in a file, while operator marks the locations of cells on the improved figures (Figure 3.2). This simple solution provides great deal of comfort for the user, as well as improved accuracy.

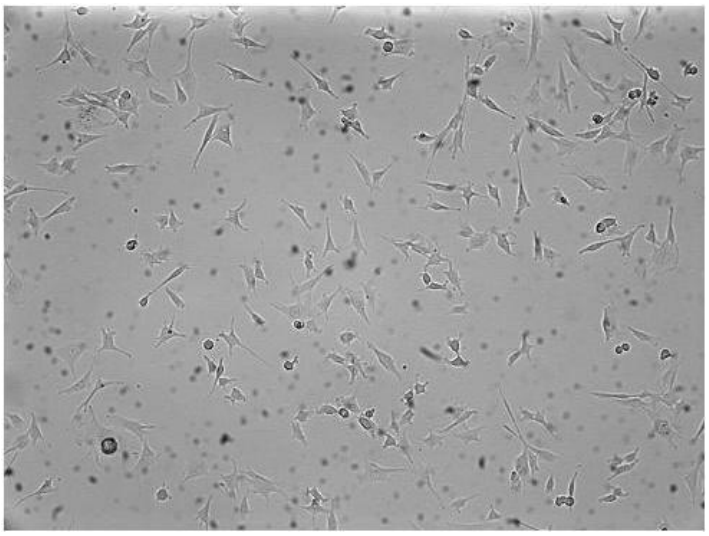

(a)

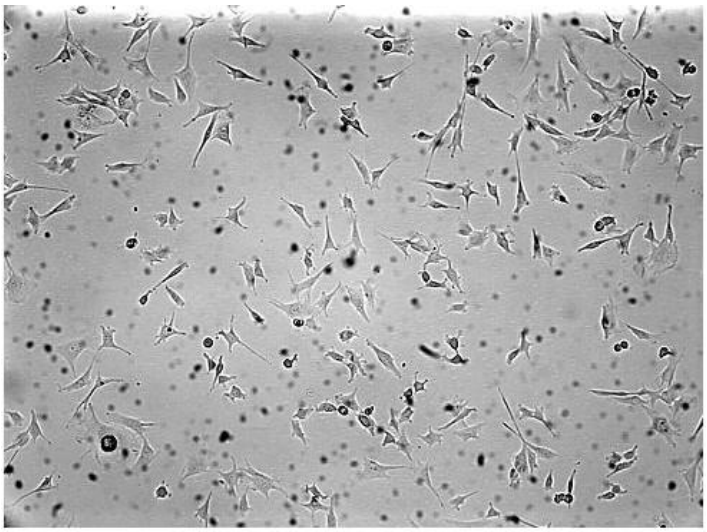

(b)

Figure 3.1. (a) Cell culture photograph (b) Improved cell culture photograph

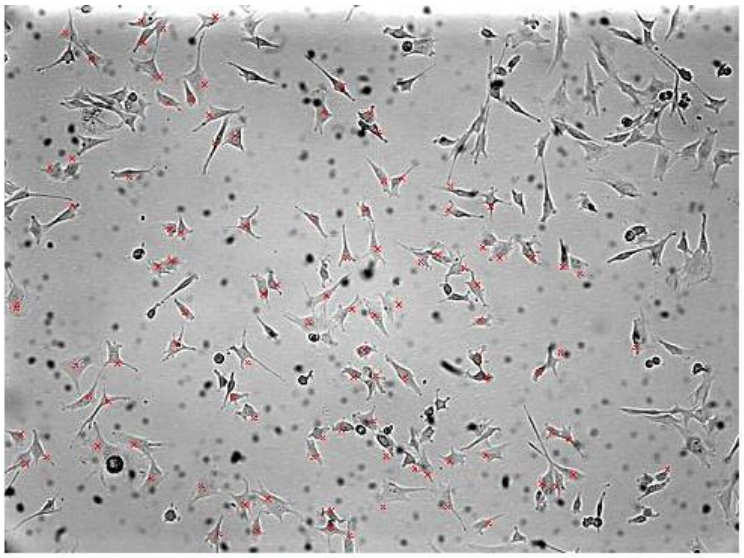

Figure 3.2. Counting cells by marking them on figure

Three experiments have been performed for different initial populations and environmental conditions. In the first one, initial population was low (1:20 proportion) and the medium was clean. In the second one, initial population was low, however cells was placed into the medium of the previous experiment after adding some nutrient to the medium. In the last experiment, cell population was even higher (1:10 proportion) while the medium was clean.

The data were gathered during three days, three times a day from three parallel flasks in order to checking the reliability of the counting process. Experimental data are provided in Appendix A.

4. MODELS

Two models are developed for modelling the population dynamics in cell cultures at the mitotic stage. The first model is a cellular automata-like micro-model allowing distributed representation of the cell population dynamics in a flask, while the second one is a nonlinear type of macro-model based on a lumped representation of the total population and the total toxicity in the flask. Since practical limitations allow only very scarce experimental data, using these limited data to develop a macro model that sufficiently well describes the overall behavior of the population dynamics is hard in general. To circumvent the lack of sufficient data for a macro-model, first, a biologically plausible CA-like model is developed based on the life cycle of an individual cell and its interactions with environment. By using the experimental data, the parameters of micro-model are tuned. Secondly, simulation results of the micro-model are used to develop a model that describes the macro behavior of the cell population analytically. This macro-model consists of sets of nonlinear, continuous time, ordinary differential equations which provide piecewise description of some relevant parts of the state-space.

4.1. Micro-Model: A Deterministic CA-like Model

Micro-model proposed here to represent the population dynamics in cell cultures at the mitotic stage is a deterministic, discrete-time discrete-space model that uses some properties of CAs. CAs were originally conceived by Ulam and von Neumann in the 1940s to provide a formal framework for investigating the behavior of complex, extended systems. In the early 50s [40], CAs were started to be thought as a possible model for biological systems, and since then they have been used to simulate various biological populations such as bacterial biofilms, plant growth, and tumor development [41–45].

CA is a discrete model which consists of a regular grid of points commonly called as *cells*. The grid can have any finite number of dimensions. Each point in CA has a neighborhood associated with itself, where this neighborhood is a set of some other grid points in the CA determined by a certain rule. Each point has a state which evolves

over the time with respect to some rules determining the next state of a cell according to this point's current state as well as the current states of the points in its neighborhood. These rules are iteratively applied as many steps as desired, and in each iteration, all updates are carried out simultaneously. In general, the rules used for the update of cell states are the same for all cells, and are time-invariant, i.e., these rules do not change over the time. Using CA, the population dynamics can be numerically analyzed to get a macroscopic view of the population by considering the microscopic view of the population, i.e., global behavior of the population is characterized by examining the properties of a cell (or a cell group) and the interactions of this cell with the other ones [46].

Although the proposed micro-model is somewhat similar to CA in spirit, still there are some important differences that need to be mentioned. In particular, the proposed micro-model differs from a classical CA model in two ways. The first difference is that in CA models, a grid locus generally represents a cell, whereas this model allows a grid locus be occupied by more than a single cell. Since a grid locus represents the location of cells instead of a cell, it is called "*locus*" instead of "*cell*", and *cell* refers to an actual biological cell in this model. The second difference is that in addition to cells, the environment also has dynamic properties in the proposed micro-model as opposed to a classical CA where only cells display a dynamic attitude, while the environment is static.

Each cell is structured with various properties like energy, division status, period of life among which the cell energy is the key property governing the other ones. The environment is composed of regular grids where each grid locus has a constant nutrient and varying toxicity value. The cells and the environment interact in two forms: Each cell takes nutrient from environment and releases some amount of toxicity to the locus it occupies. Thus, micro-model consists of two main building blocks, one of which comes from the representation of the environment (flask) with its dynamicity, and the other one comes from the representation of the cell with its dynamicity. A detailed explanation of these two main blocks is provided in the next sections.

4.1.1. Representation of the environment and its dynamics

In the proposed micro-model, the flask is represented by a $n \times n$ matrix, which corresponds to a regular grid. Each mesh of this grid is called *locus*, and is represented by an entry of the $n \times n$ matrix, say the $(i, j)^{\text{th}}$ entry where $i = 1, 2, \ldots, n$, $j = 1, 2, \ldots, n$.

Each locus has the following the properties:

- Cell accommodation capacity per locus: The observations of the flask reveal the fact that as the population increases, cells can be placed on the top of other cells (Figure 4.1). Thus, a locus of the grid, represented by the $(i, j)^{\text{th}}$ entry of the $n \times n$ matrix, can host to a maximum number of cells, denoted by z, and z is selected to be the same all loci, i.e., for all elements of the $n \times n$ matrix.

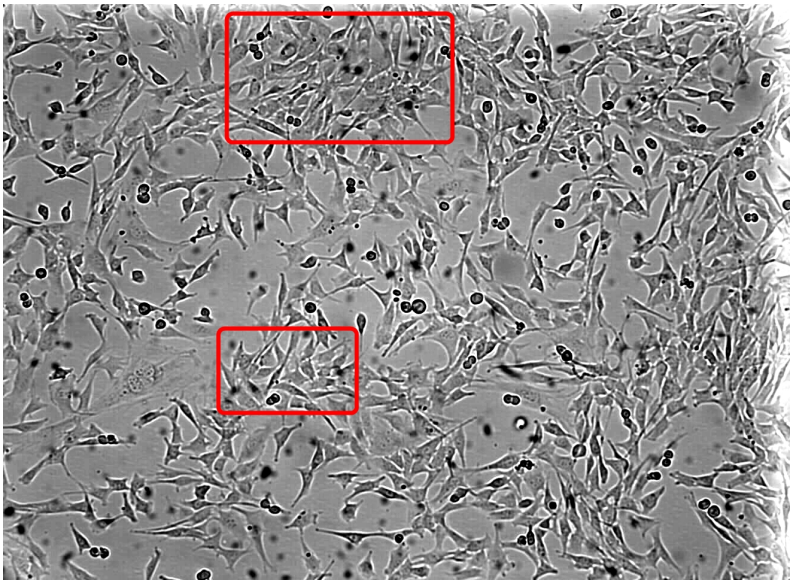

Figure 4.1. Microscopic view of the flask where multiple cells are co-located

- Nutrient hosting capacity per locus: In experiments, the medium in the flask is initially rich in nutrition. Moreover, the entire duration of the experiment, which is approximately three days, is relatively short to lead a substantial decrease in the initial nutrition amount. Thus, in the design of the micro-model, it is assumed

that nutrition remains constant over time. In particular, it is assumed that at each locus, there is a nutrition supply which can feed all cells in this locus with a certain fixed amount of nutrient per cell denoted by A, which does not change over time.

- Toxicity: Each locus has a certain amount of toxicity at time k denoted by $x_{i,j}(k)$. Contrary to the nutrition at each locus, the toxicity at a locus changes over time since each cell releases toxicity to the locus it occupies and the toxicity of each locus diffuses to the other loci in its neighborhood. It must be noted that since the flask is an isolated environment with no interaction over its boundaries, there is no leakage of toxicity from the flask. Thus, the entire toxicity in the flask cannot decrease, i.e., $\sum_{\forall(i,j)} x_{i,j}(k)$ is a non-decreasing function of time k.

As mentioned earlier, the environment in this micro-model is represented as a dynamic system as opposed to CA models. The dynamicity of the environment arises from the fact that toxicity at each locus changes. Next, the mathematical formulation of the two processes, namely the release of toxicity by cells and the diffusion of toxicity among the loci, will be explained.

Each cell releases a certain amount of toxicity which is determined by the amount of the nutrition taken from the locus. In particular, the following relationship holds

$$x^r_{i,j,l}(k) = \beta A; \tag{4.1}$$

where $x^r_{i,j,l}(k)$ denotes the amount of the toxicity released by l^{th} cell in $(i,j)^{\text{th}}$ locus, β is the constant, and A is the constant amount of nutrition taken by a cell at each time step. Since each locus can accommodate many cells, indeed at most z cells, the total amount of released toxicity $x^r_{i,j}(k)$ at $(i,j)^{\text{th}}$ locus at time k can be written as

$$x^r_{i,j}(k) = \sum_{l=1}^{m_{i,j}(k)} x^r_{i,j,l}(k) \tag{4.2}$$

where $m_{i,j}(k)$ is the total number of the cells located at the $(i,j)^{\text{th}}$ locus at time k. It

should be noted that $m_{i,j}(k) \leq z,\ \forall(i,j,k)$. The release of toxicity always increases the toxicity amount in each locus whereas the diffusion process may increase or decrease the toxicity amount in each locus depending on the toxicity amount of this locus' neighborhood.

Diffusion is the movement of mobile particles that migrate from regions with higher concentration to those with lower concentration. In the micro-model, toxicity diffuses from a locus to neighboring loci with less toxicity. In particular, the diffusion of the total toxicity $x_{i,j}(k)$ at the $(i,j)^{\text{th}}$ locus will be from this locus to its neighboring loci with lower toxicity than $x_{i,j}(k)$. Similarly, the $(i,j)^{\text{th}}$ locus will receive toxicity from its neighboring loci whit higher toxicity than $x_{i,j}(k)$. If the space coordinates and time are represented as continuous, the diffusion process can be described by the following partial differential equation (PDE)

$$\frac{\partial x(i,j,t)}{\partial t} = D\left(\frac{\partial^2 x(i,j,t)}{\partial i^2} + \frac{\partial^2 x(i,j,t)}{\partial j^2}\right) \tag{4.3}$$

where t denotes the continuous time, D the diffusion coefficient that determines the speed of diffusion and $x(i,j,t)$ is the total toxicity at position (i,j) at time t [47]. Since in the micro-model model, time and space are discrete, a discretized version of (4.3) can be used to describe the diffusion process. In particular, *forward-time centered-space* (FTCS) method is used to discretize (4.3). The corresponding discrete-time discrete-space diffusion equation applicable to the micro-model

$$\begin{aligned} x(i,j,k+\Delta k) = {} & \frac{D\Delta k}{(\Delta i)^2}\left(x(i+\Delta i,j,k) + x(i-\Delta i,j,k)\right) \\ & + \left(1 - \frac{2D\Delta k}{(\Delta i)^2} - \frac{2D\Delta k}{(\Delta j)^2}\right) x(i,j,k) \\ & + \frac{D\Delta k}{(\Delta j)^2}\left(x(i,j+\Delta j,k) + x(i,j-\Delta j,k)\right) \end{aligned} \tag{4.4}$$

where Δi (resp. Δj) is the differences between the abscissas (resp. the ordinates) of two neighboring loci, and Δk is the time-step,of the diffusion process. Hence, between time $k+1$ and time k, there are $1/\Delta k$ diffusion processes. Δk needs to selected properly to ensure the convergence of the discrete diffusion equation in (4.4). In particular, it

can be chosen according to the Courant condition, which is a necessary condition for the convergence of the discretized partial differential equations like the one in (4.4). According to the Courant condition, Δk needs to satisfy

$$\Delta k \leq \frac{1}{2D}\left(\frac{1}{(\Delta i)^2}+\frac{1}{(\Delta j)^2}\right) \tag{4.5}$$

Since in the proposed micro-model diffusion process takes place between a locus and its nearest neighbors $\Delta i = \Delta j = 1$. Thus, in the micro-model, (4.4) reduces to

$$\begin{aligned} x_{i,j}(k+\Delta k) = {} & D\Delta k\left(x_{i+1,j}(k)+x_{i-1,j}(k)\right)+\left(1-4D\Delta k\right)x_{i,j}(k) \\ & + D\Delta k\left(x_{i,j+1}(k)+x_{i,j-1}(k)\right) \end{aligned} \tag{4.6}$$

Since the flask is an isolated environment with no interaction across its boundaries, there is no leakage of toxicity from the flask to an external system. To include this fact in the micro-model, some boundary conditions are imposed upon the diffusion equation in (4.6). This is achieved by expanding the $n \times n$ matrix by adding two columns and two rows according to the following boundary conditions:

- $x_{0,j}(k) = x_{1,j}(k),\ \forall(j,k)$
- $x_{n+1,j}(k) = x_{n,j}(k),\ \forall(j,k)$
- $x_{i,0}(k) = x_{i,1}(k),\ \forall(i,k)$
- $x_{i,n+1}(k) = x_{i,n}(k),\ \forall(i,k)$

Since diffusion cannot take place between two loci with the same amount of toxicity, these boundary conditions prevent the leakage of toxicity from the flask.

So far, mathematical descriptions of the two processes that contribute to accumulation of toxicity at a given locus are provided. However, these two processes are described separately as if they never act on the toxicity simultaneously. Next, to obtain their cumulative effect on the toxicity at a locus, the overall mathematical description of the system that combines these two processes will be explained. To this end, it is

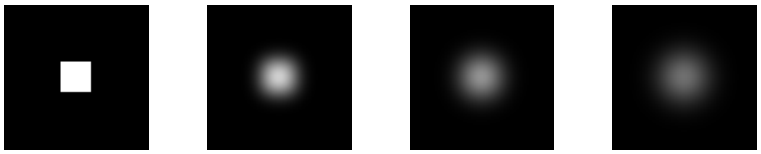

Figure 4.2. Illustration of the diffusion process

noted that the diffusion of toxicity occurs at times $k, k+\Delta k, k+2\Delta k, \ldots$, and the release of the toxicity occurs at times $k, k+1, k+2, \ldots$. Keeping this in mind, one can combine (4.2) and (4.6) to get an overall mathematical description for the micro-model as follows:

$$x_{i,j}(k+\ell\Delta k) = \begin{cases} D\Delta k\left(x_{i+1,j}(k)+x_{i-1,j}(k)\right)+\left(1-4D\Delta k\right)x_{i,j}(k) \\ \quad +D\Delta k\left(x_{i,j+1}(k)+x_{i,j-1}(k)\right), \qquad \text{if } \ k+\ell\Delta k \text{ is not an integer} \\ \\ D\Delta k\left(x_{i+1,j}(k)+x_{i-1,j}(k)\right)+\left(1-4D\Delta k\right)x_{i,j}(k) \\ \quad +D\Delta k\left(x_{i,j+1}(k)+x_{i,j-1}(k)\right)+\sum_{l=1}^{m_{i,j}(k)}\beta A, \qquad \text{otherwise} \end{cases}$$

where $\ell = 0, 1, \ldots$.

4.1.2. Representation of cells and their dynamics

A cell has a complex nature for which it seems to be an elusive task to obtain an analytically tractable model. In this model, only certain properties of cells are considered.

- Energy: Each cell has a total energy. In our model, energy of a cell is taken as the sole factor leading the growth process. In this model, energy somewhat accounts for other possible variables such as size and age, which are commonly used in other models in the literature. Growth of a cell is modelled as increase of its total energy. The total energy of a cell increases due to the nutrient taken in and some of this energy is spent on the remediation of damages caused by the

toxicity at the cell's locus. The energy level of a cell determines whether the cell becomes mitotically active or not, as well as whether it expires or not.

- Release of Toxicity: Since each cell takes in some nutrient from the environment and converts it into energy, as a by-product of this metabolic process it also produce some waste, i.e., toxicity. Each cell releases its toxicity as expressed in equation 4.1 to the locus it occupies.
- Cell Cycle: Although a cell cycle consists of many stages (Figure 2.1), only two major stages of this cycle, namely the interphase and the mitotic phase, are considered in this model. During the interphase of a cell cycle, which includes the G1, S, G2 stages of a cell cycle, the cell grows up as a result of energy accumulation. When the accumulated energy reaches a certain threshold, the interphase period ends, and the mitotic phase (M phase) of the cell cycle starts. The mitotic phase is a complex stage which is determined both by the internal state of the cell (e.g. accumulated energy) and the external conditions imposed by the environment. In particular, besides a certain amount of energy, for a cell to be able to divide into two daughter cells, certain environmental conditions need to be satisfied as well. The most important environmental influence that can prevent the cell from starting the division process is due to so-called contact-inhibition behavior, the cells' way of avoiding dense accommodation. If there is sufficient space in the flask to accommodate two new daughter cells. The cell goes through the division process, being called mitotically active. Otherwise, the division process does not start and the cell becomes quiescent, i.e., the G0 phase of the cell cycle starts. In this phase, the metabolic activities of the cell like feeding and producing waste runs at the basal level. This stage continues until the necessary environmental conditions are satisfied, for example until the necessary space to accommodate two new daughter cells arises. When the necessary environmental conditions are satisfied, the cell becomes mitotically active again.

In the presented micro-model, growth, division and death dynamics of a cell are ruled by some energy functions. Each cell has a energy budget. Each cell takes a constant amount of nutrient A leading to an increase in the total energy of the cell, and releases a certain amount of toxicity to its locus. In our model, the toxicity in

the environment can be viewed as the variable that implicitly captures the influence of the cell population's density on the lifespan of the cell culture. Each cell spends some energy to remediate the damage caused by the toxicity at its locus.The amount of energy expenditure E^{rem} corresponding to the efforts to remediate the damage on the cell caused by the local toxicity x at a given time step can be expressed as a function of x which is expected to satisfy the following conditions:

- If $x = 0$, we also have $E^{rem} = 0$
- E^{rem} is a nondecreasing function of x
- For large values of x, E^{rem} saturates, i.e., $\lim_{x\to\infty} E^{rem} = c$, where $c < \infty$ is a constant value.

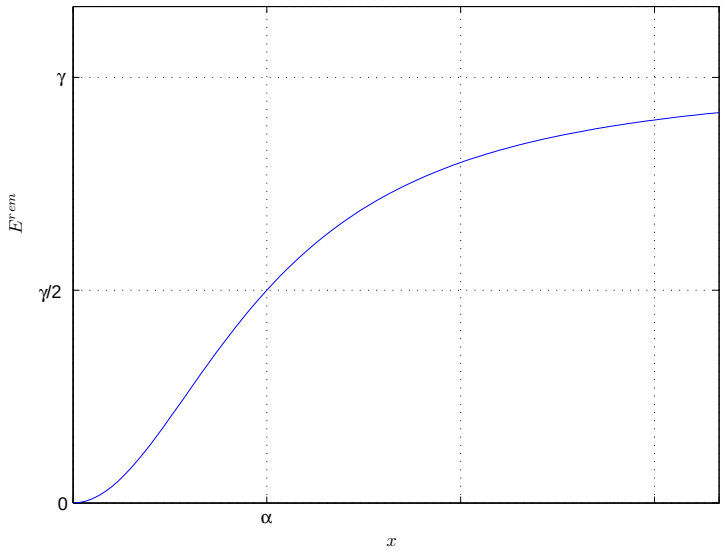

Figure 4.3. Energy expenture as a response to damage by toxicity

A simple, analytic function satisfying all these three conditions (Figure 4.3) can be written as follows:

$$E^{rem} = \frac{\gamma A x^2}{\alpha^2 + x^2} \tag{4.7}$$

where γ, α and A are parameters to be appropriately chosen in order to provide plausible population dynamics. It is noted that depending on the toxicity at its locus,

the energy harvested by a cell may or may not be enough to provide $E_{i,j}^{rem}(k)$, the energy necessary to remediate the damage created by the toxicity $x_{i,j}(k)$ at time k. Consequently, if $E_{i,j}^{rem}(k) > A$, the total energy of any cell at locus (i, j) will decrease.

The energy update relationship of a cell depends on the division phase of the cell, in particular, whether the cell is mitotically active or quiescent. If a cell is mitotically active, it keeps accumulating energy until the level sufficient for division. The energy update equation for such a cell is given by

$$E_{i,j,l}(k+1) = E_{i,j,l}(k) + \left(A - \frac{\gamma A x_{i,j}(k)^2}{\alpha^2 + x_{i,j}(k)^2}\right) \tag{4.8}$$

where $E_{i,j,l}(k)$ is the total energy of the l^{th} cell at the $(i, j)^{\text{th}}$ locus at time k. However, if a cell is in the quiescence phase, its metabolism runs at a basal level, i.e., the cell never aims to grow and just preserves its current size. This behavior is modelled as that if the harvested energy from the available nutrient in the environment is enough to remediate the damage caused by the local toxicity, i.e. $A \geq E_{i,j}^{rem}(k)$, the cell stays at the same energy level. Otherwise its total energy decreases. In particular, the energy update for a cell in in quiescence state is given by

$$E_{i,j,l}(k+1) = \begin{cases} E_{i,j,l}(k) & \text{if } \ A \geq E_{i,j}^{rem}(k) \\ \\ E_{i,j,l}(k) + \left(A - \frac{\gamma A x_{i,j}(k)^2}{\alpha + x_{i,j}(k)^2}\right) & \text{if } \ A < E_{i,j}^{rem}(k) \end{cases} \tag{4.9}$$

This energy update equation of the cell in quiescence state implies that cells at loci with low toxicity can preserve their total energy, while those at loci with higher toxicity the damage of which cannot be compensated by the harvested energy start losing their total energy. When a cell, whether quiescent or not, continues losing energy, such that the total energy eventually drops below a certain threshold the cell dies (Figure 4.4).

A cell continues growing, i.e., the stay in the interphase, until it has sufficient total energy to undergo division. When the total energy of a cell is sufficient for division and the environmental conditions are appropriate, it divides into two daughter cells

with initial energies obtained by equally sharing the mother cell's total energy.

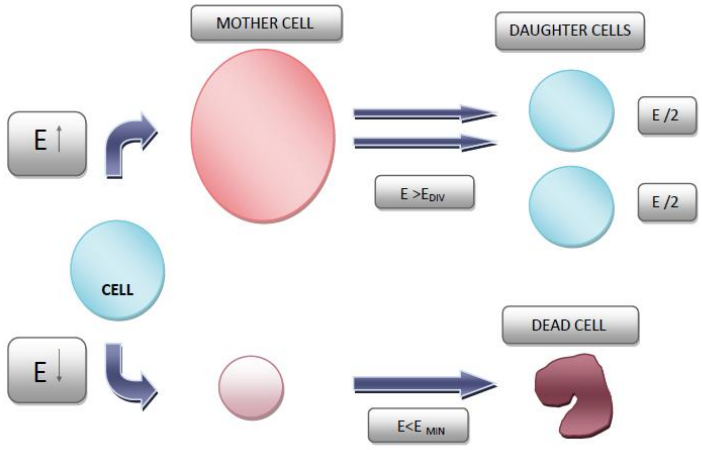

Figure 4.4. Energy functions of division and death processes

The placement of the off-springs arriving at the end of the mitotic division needs explanation. In cell cultures, cells gather information from their environment. This communication is especially important when the daughter cells being placed. In particular, these offsprings end up to some neighborhood of the former mother cell with relatively low population density. In our model, the toxicity of any locus is used as an indicator of the population density at the locus. Low toxicity means relatively low population density at and around this locus. Consequently, in this model new-born cells are placed at loci with lower toxicity. If each of the eight neighboring loci and the locus of the mother cells are already occupied by the maximum number (z) of cells, the mother cell postpones its division process and goes into the quiescence state (G0) until some neighboring loci turn suitable for offsprings. This strategy accounts for the contact inhibition behavior of the cells.

4.1.3. Parameter Tuning of the Micro-Model

There are many parameters in the micro-model to be tuned in order to obtain population dynamics similar to the experimental data. Some of these parameters can

be estimated from the experimental data, while others need to be adjusted by some heuristic method in order to render the simulation results similar to the experimental results.

- The square flask is represented as an $n \times n$ matrix of loci of the approximate size of a single cell. Thus n^2 can be calculated as the ratio of the flask area to the average cell area. In our experiment flask of area 25 cm^2 have been used and the average area of C2C12 cell is 1500 μm^2, hence $n^2 \simeq 1.67 \times 10^6$. Hence, we set $n = 1300$.
- The maximum number of cells that each locus can accommodate (z) is chosen based on practical considerations related to the algorithm. The maximum number of new cells that can be placed on any locus at a single step is 9, because the mother-cells can only be at the 8 nearest neighbor loci and at the locus under consideration, $z = 9$ has been chosen in order to give all of them equal opportunity.
- In our model, we take $A = 1$ energy unit/step, and the time step as 15 minutes for practical purposes. Since by an appropriate scaling, these two parameters A and the time step can be simply adjusted to different environmental conditions, the current selections do not incur any loss of generality to the model.
- Doubling time is the time needed for the population size to reach twice its initial value. When the flask has no initial toxicity and has a diluted population, doubling time is determined as 18 hours from the experimental data. Hence doubling time is estimated as $k_{double} = 72$ time steps = 18 h/15 min
- The division energy E^{div} is estimated from data obtained from an experiment with low initial population and starting with a clean flask. Since the initial population is assumed to have a low density, which is approximately %0.3, and diffusion process is fast enough to spread the toxicity generated by low population, the average toxicity in environment can be assumed to be negligible, i.e., $\bar{x} \approx 0$ where $\bar{x}$ denotes the average toxicity in the environment. Using this assumption,

average energy evolves as

$$\bar{E}(k+1) = \bar{E}(k) + A \tag{4.10}$$

$$= \bar{E}(k) + 1 \tag{4.11}$$

where $\bar{E}(k)$ denotes the average energy, and (4.11) follows from choosing $A = 1$. $\bar{E}(0)$, the average initial energy of the population, is assumed as $\bar{E}(0) = E^{div}/2$, i.e., the average initial energy is equal to the half of division energy. Using this assumption in (4.11), we get

$$\bar{E}(k) = \frac{E^{div}}{2} + k \tag{4.12}$$

Finally, using the fact that at the doubling time of the population, each cell divides itself into two daughter cells, i.e., the average energy at the doubling time is equal to the division energy $\bar{E}(k_{double}) = E^{div}$ in (4.12),

$$\bar{E}(k_{double}) = \frac{E^{div}}{2} + k_{double} \tag{4.13}$$

$$E^{div} = \frac{E^{div}}{2} + k_{double} \tag{4.14}$$

The division energy is calculated as $E^{div} = 144$.

- The time-step between two diffusion processes is selected as $0.4/D$ to ensure that the Courant condition in (4.5) is satisfied and thus the algorithm converges.

The rest of the parameters involved in micro-model such as $\alpha, \beta, \gamma, E_{min}$ cannot be deducted from the experimental data analytically. Thus, they are heuristically adjusted in order to obtain simulation results close to the experimental observations.

4.2. Macro-Model: A 2-Dimensional Nonlinear Dynamic System

A typical representation for a non-linear dynamic system can be given by $\underline{\dot{X}} = \underline{F}(\underline{X})$ where $\underline{F}(\underline{X})$ is a non-linear non-autonomous function, and $\underline{X} = (X_1, X_2, \ldots)$ is the state vector. The state variables that constitute the state vector of a deterministic system has to satisfy two important conditions:

- They have to span the whole state-space
- Trajectories of state variables corresponding to different initial conditions should not intersect

One of the simplest and most popular model for growth dynamics of organisms is the logistic equation, first proposed by Verhulst [5].

$$\dot{N} = \lambda(1 - N/K)N \tag{4.15}$$

This models is based on the assumptions that available resources are limited, that the per capita birth and mortality rates depend on the population size and that an optimal population size K, i.e. carrying capacity, exists [3]. It is represented as a non-linear dynamic system with a single state variable which is the population size.

In this part of the project, the task is to match a set of coupled differential equations to the micro-model results. The first step is the specification of the state variables. The most natural candidates are the total population N and total toxicity x. Next, the differential equations governing these state variables have to be determined and it has to be checked whether these variables indeed span a state space. The differential equation expressing the change of total population is expected to be similar to the Verhulst model (4.15). However, unlike the Verhulst model, there has to be a dependence on the total toxicity accumulated in the environment. On the other hand, the differential equation expressing the change in the total toxicity is rather trivially derived from the micro-model which gives the change in the total toxicity as proportional to the present population size. Thus a set of differential equations of the

following form are expected,

$$\dot{N} = f(N, x) \tag{4.16}$$

$$\dot{x} = \beta N \tag{4.17}$$

where $f(N, x)$ is an unknown function that needs to be estimated from the micro-model data.

Figure 4.5(a) shows the (N, x) phase portrait obtained from the micro-model data with different initial conditions $(N(0), x(0))$. As can be seen in the figure, phase trajectories corresponding to different initial conditions intersect indicating that N and x actually do not constitute a full set of state variables.

However, trajectories corresponding to zero initial toxicity $(x(0) = 0)$ do not intersect (Figure 4.5(b)). This finding implies that a macro-model corresponding to this special initial condition can be derived. For the validity of such a 2-d macro-model a further assumption is necessary, namely about the initial (and subsequent) homogeneity of the population distribution, since with total population size and total toxicity as the macro state variables, different heterogeneous distributions would not be distinguishable although they would give rise to completely different dynamics.

When initially there is no cell in the flask, i.e., $N(0) = 0$, obviously the total population must always remain zero implying $\dot{N} = 0$. Thus, $f(N, x)$ has to have the form $f(N, x) = Ng(N, x)$.

4.2.1. Tuning the Macro-Model

Now, the function $\dot{N} = f(N, x) = Ng(N, x)$ has to be estimated such that it fits the phase-portrait obtained from the micro-model results. Observing that this phase-portrait exhibits qualitatively different behavior in different regions (Figure 4.6) it has been decided to fit a separate model to the regions of growing population, stagnating population and decreasing population, while the region corresponding to low initial

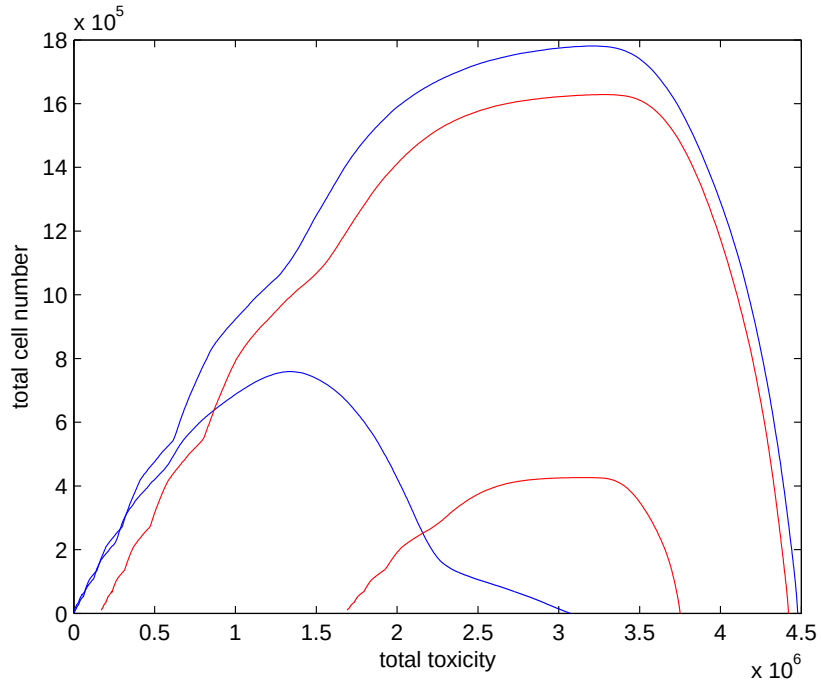

(a)

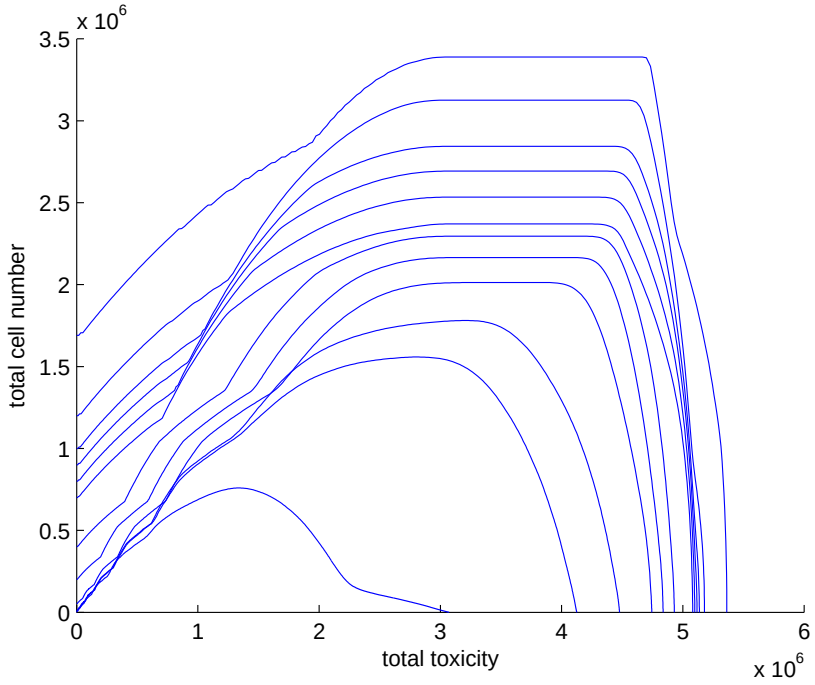

(b)

Figure 4.5. Phase portraits for (a) different initial conditions including nonzero initial toxicity $x(0) \neq 0$ (b) different initial conditions with zero initial toxicity $x(0) = 0$

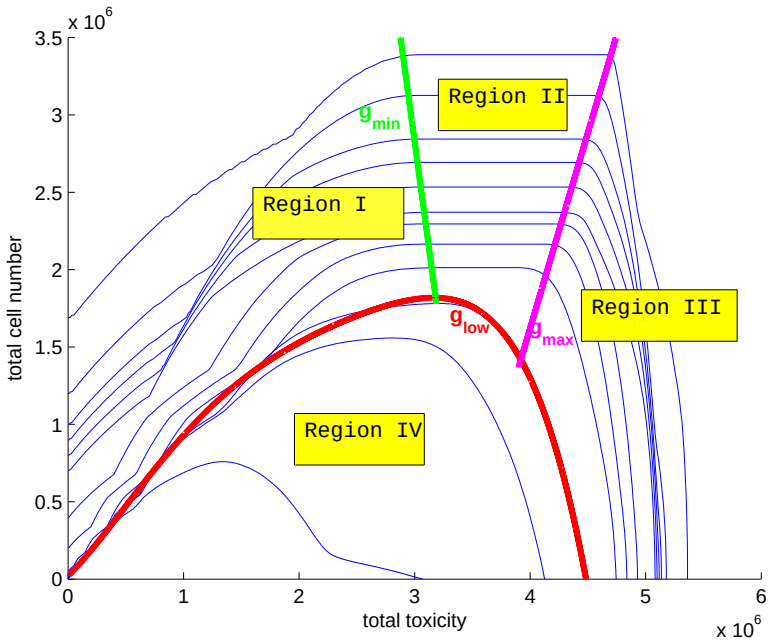

Figure 4.6. Phase portrait regions with different qualitative behavior

population, which does not constitute a state space, is excluded from the macro-model. The boundaries between these regions have been manually placed and their equations have been estimated as follows:

$$g_{min}(x) = 19.418 \times 10^6 - 5.53x \tag{4.18}$$

$$g_{max}(x) = -8.4909 \times 10^6 + 2.528x \tag{4.19}$$

$$\begin{aligned} g_{low}(x) = &-1.8186 \times 10^{-26}x^5 + 1.6238 \times 10^{-19}x^4 - 5.2050 \times 10^{-13}x^3 \\ &+ 5.4139 \times 10^{-7}x^2 + 0.7458x + 1.8842 \times 10^4 \end{aligned} \tag{4.20}$$

Phase portrait fitting in these regions have resulted in the following macro-models:

- Region I: If the state variables N and x satisfy

$$g_{low}(x) < N < g_{min}(x) \tag{4.21}$$

the population is rising. With an appropriate modification of the Verhulst model and adjustment of parameter K_{rise} by trial-and-error the following system of ODEs is obtained for region I:

$$\dot{N} = K_{rise} N(g_{min}(x) - N) \tag{4.22}$$

$$\dot{x} = \beta N \tag{4.23}$$

- Region II: If the state variables N and x satisfy

$$N > g_{low}(x) \tag{4.24}$$

$$N > g_{min}(x) \tag{4.25}$$

$$N > g_{max}(x) \tag{4.26}$$

the population size stagnates. Hence, the system of ODEs governing region II can be written as follows:

$$\dot{N} = 0 \tag{4.27}$$

$$\dot{x} = \beta N \tag{4.28}$$

- Region III: If the state variables N and x satisfy

$$g_{low}(x) < N < g_{max}(x) \tag{4.29}$$

the population is dropping. With an appropriate modification of the Verhulst model and adjustment of parameter K_{drop} by trial-and-error the following system of ODEs is obtained for region III:

$$\dot{N} = K_{drop} N(g_{max}(x) - N) \tag{4.30}$$

$$\dot{x} = \beta N \tag{4.31}$$

- Region IV: If the state variables N and x satisfy

$$N < g_{low}(x) \tag{4.32}$$

the system must have started with low initial population. Because of the low density of cells (hence the long distances between cells) the distribution of toxicity remains mostly nonuniform for the diffusion rate adjusted to that of the medium used in the experiments. Consequently, the system does not lend itself to a representation in terms of the considered macro-variables, namely the total toxicity and the total population. So no macro-model has been developed for this part of the state space (as a matter of fact, this region does not constitute a space space even under zero initial toxicity assumption). Theoretically, for a medium with very high diffusion rate such a region would not exist.

5. RESULTS AND DISCUSSION

5.1. Experimental data

Cell culture population growth experiments have been performed on three parallel flasks which have provided rather consistent data (Figure 5.1)(see Appendix A). Because counting very crowded cell populations creates serious practical problems experiments have been limited to three days. Therefore, the expected saturation and subsequent decrease of population due to toxicity could not be observed in these experiments. However, in the experiment the result of which is given in Figure 5.1(c) starting with high initial population at least the decrease of growth rate has been observed as population became large enough.

5.2. Simulation results from the micro-model

Figure 5.2 shows the simulation results obtained from the micro-model the parameters of which have been tuned to the experimental outcomes. Each graph is the comparison of simulation results and experimental data obtained from different experimental setups. For the second experiment in which the medium has initial toxicity, the simulations of the micro-model is also started with an initial toxicity. This toxicity amount is also determined by simulation such that simulation is started with initially clean medium, and the total initial toxicity after three days (288 time steps) is calculated. The tuned parameter set is given in Table 5.1.

Table 5.1. Parameter values of the micro-model as tuned to the experimental data

β	D	E_{min}	α	γ
0.01	1	40	$3\sqrt{10}$	30

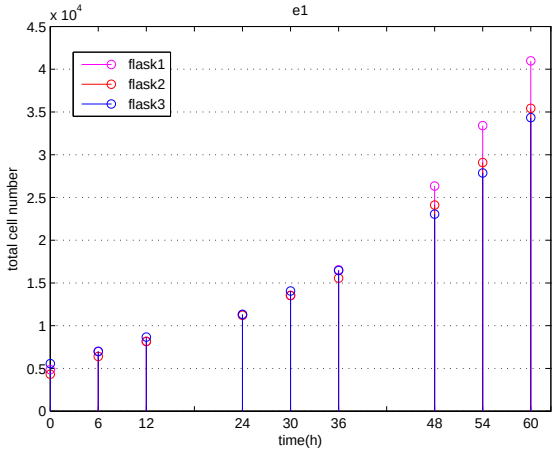

(a)

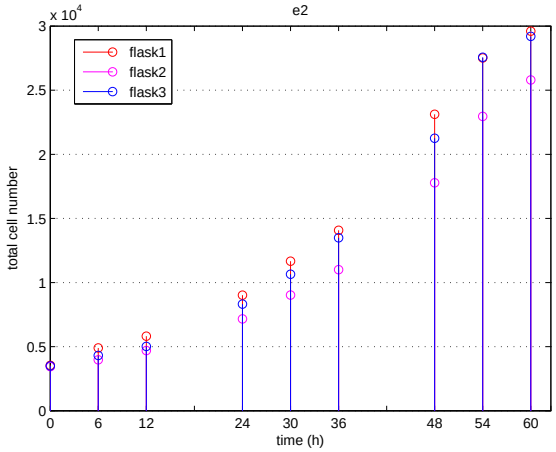

(b)

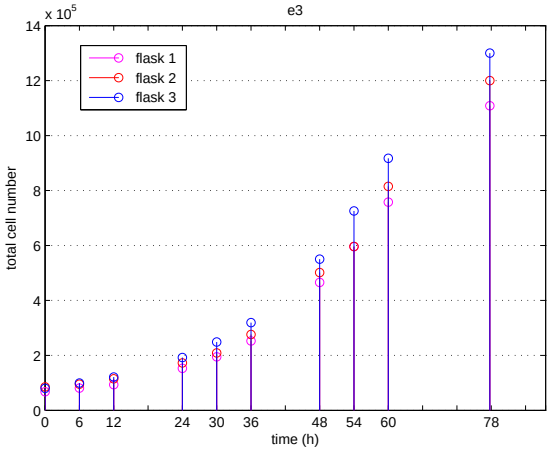

(c)

Figure 5.1. Experimental data from the (a) 1^{st} experiment (initially low populated, clean medium) (b) 2^{nd} experiment (initial low population, initial toxicity) (c) 3^{rd} experiment (initially high populated, clean medium)

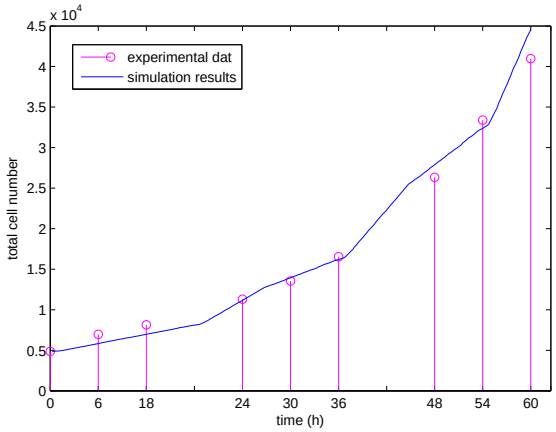

(a)

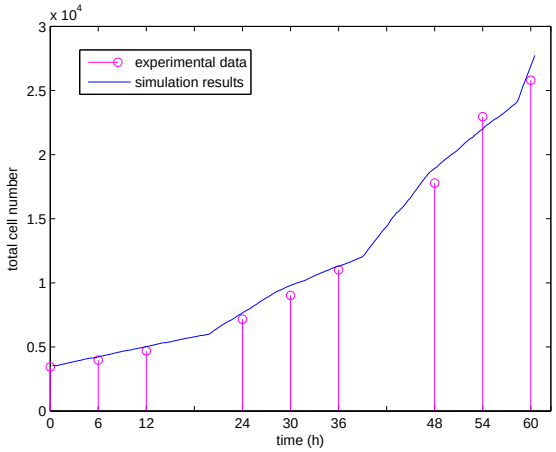

(b)

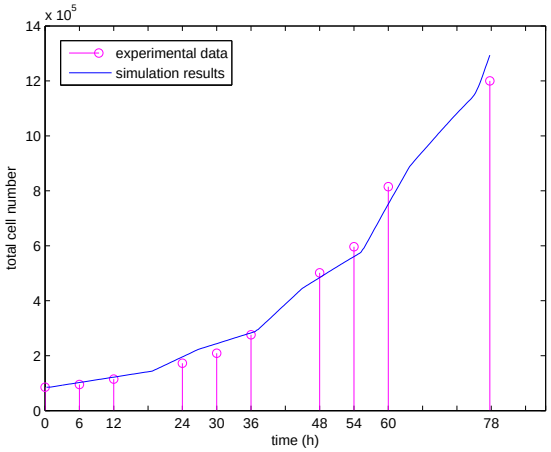

(c)

Figure 5.2. Micro-model simulation results versus experimental data (a) from the first experiment (b) from the second experiment (c) from the third experiment

5.3. Simulation results from the macro-model

The two dimensional macro-model has been obtained by piecewise phase-portrait fitting to three different sub-regions of the N-x state space data obtained from the micro-model. Although guided by some theoretical knowledge about the population dynamics, phase-portrait fitting has been accomplished basically by trial-and-error. Since the macro-model is only feasible for systems with high initial population, the macro-model results are compared only to the corresponding experimental data given in Figure 5.1(c).

Table 5.2. Parameter values of the macro-model as tuned to the simulation results obtained from micro-model

K_{rise}	K_{drop}
$5.5\ 10^{-10}$	$3\ 10^{-8}$

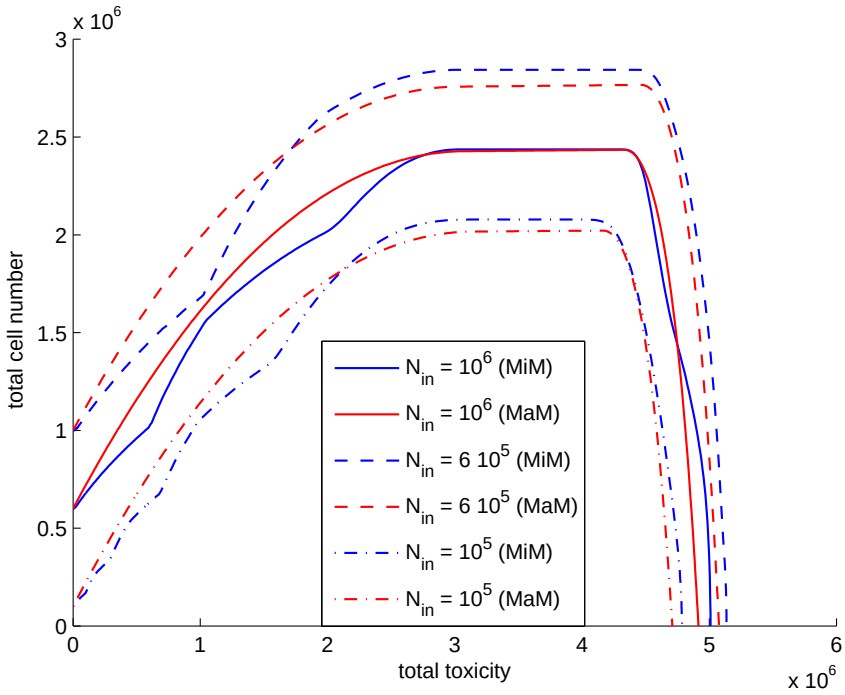

Figure 5.3. Phase portraits: macro-model versus micro-model simulation results

As it can be seen in Figure 5.3, the piecewise macro-model given by the system of equations in (4.22)-(4.23), (4.27)-(4.28), and (4.30)-(4.31) provide phase trajectories

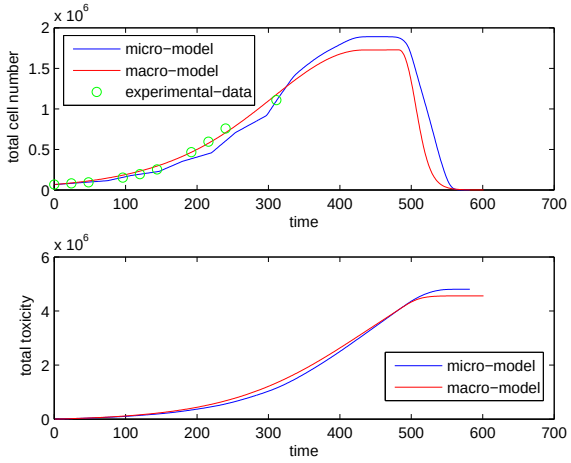

(a)

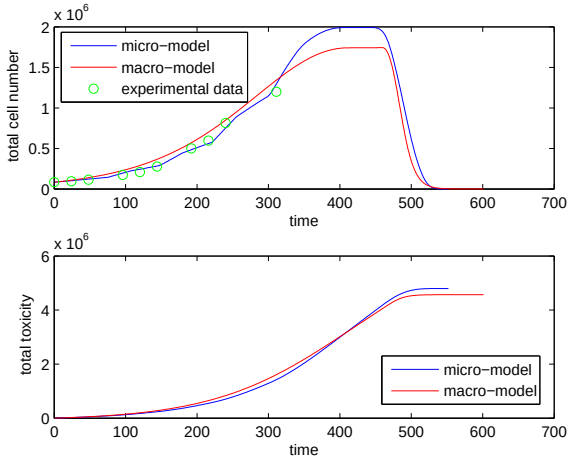

(b)

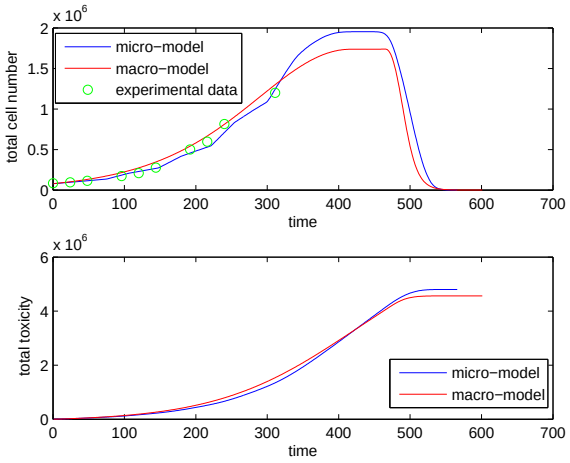

(c)

Figure 5.4. Micro- and macro-level simulation results and experimental data from the third experiment from (a) the first flask (b) the second flask (c) the third flask

in good agreement with those obtained from the micro-model. Figure 5.3 give the state variables as a function of time. Also these figures demonstrate that -under the assumptions of zero initial toxicity, high enough and homogeneously distributed initial population- the macro-model is capable of predicting the micro-model results with rather high confidence.

6. CONCLUSIONS

The aim of this thesis was to develop models that would be useful for the analysis and prediction of population dynamics in cell cultures. To this end a CA-like biologically plausible micro-model and an average macro-model of the form of nonlinear differential equation system have been developed, which constitute the main contribution of this thesis.

The proposed micro-model is actually rather different than the classical CA formalism used in other fields in the sense that it accounts for the dynamics of the environment (toxicity) as well. Also the contact inhibition behavior of real cells has been incorporated into the model. As a specific example, the parameters of this model have been tuned in order to model the population dynamics of C2C12 cell cultures at the mitotic stage by using the experimental data gathered from C2C12 cell cultures. However, C2C12 cells start to differentiate after the base of the flask is filled. Therefore, experimental data about the population decay and stagnation cannot be obtained experimentally. As a matter of fact, this part of the model is not applicable to C2C12 cells. Comparison of simulation results with the experimental data reveals that the developed micro-model is capable of tracking the population growth dynamics of C2C12 cell cultures at the mitotic stage, and is also able to provide a qualitatively correct overall population behavior. In order to see whether the developed micro-model can track the population decay patterns, further research needs to be carried out for cell cultures which do not exhibit differentiation, such as tumor cell cultures. Since the proposed micro-model tracks the growth pattern of C2C12 cell cultures satisfactorily, the micro-model is expected to have similarly good tracking capability for other cell cultures having mitotic stages similar to the C2C12 cell cultures, as long as the parameters of the micro-model are tuned according to the experimental data collected from the respective cell cultures. Another advantage that offered by the proposed biologically plausible micro-model is the fact that it provides a framework for studying the intercellular interactions, as well as the interactions between the cells and their medium.

The advantage of an analytical macro-model in the form of a set of differential equations is the fact that it can be analyzed theoretically without numerical simulation. However, still the parameters of this macro-model need to be tuned, where this task is achieved by using the numerical results obtained through the micro-model. Hence, this parameter tuning process of the macro-model can be viewed as obtaining a macro lump-parameter model from a given distributed-parameter model. Although the macro-model developed in this thesis is in some sense similar to Verhulst's logistic equation, unlike the latter, it uses two state variables along with the additional restrictions of zero initial toxicity and homogeneously distributed high initial population. The release of these restrictions may constitute interesting research directions for further studies.

Besides the two models, this thesis has also resulted in a by-product, which is a software-based aid for counting the total number of cells in a cell culture. This software takes cell culture photos as an input and improves the visibility of individual cells by appropriate image processing. Furthermore, it allows the operator to mark the cells he/she has counted by a cross. This method allows a more reliable and comfortable counting tool for laboratory personal.

APPENDIX A: Experimental Data

In this appendix, data obtained from experiments are provided. Three experiments are performed for different initial populations and environmental conditions.

- First experiment: Initial cell population is low (1:20 proportion), and medium is clean, i.e., there is no initial toxicity in the medium.
- Second experiment: Initial cell population is low (1:20 proportion), and medium is not clean, i.e., there is some initial toxicity in the medium.
- Third experiment: Initial cell population is high (1:10 proportion), and medium is clean, i.e., there is no initial toxicity in the medium.

Cell numbers are counted for three days, and three times a day from three parallel setups in order to test the reliability of counting process. In the last experiment, an additional counting is carried out at the end of the experiment by the traditional method described in Chapter 3.2.

Table A.1. Data from the 1st experiment

time (h)	1st flask	2nd flask	3rd flask
0	5563	4320	4867
6	7008	6406	6961
12	8672	8172	8141
24	11328	11219	11305
30	14063	13516	13547
36	16445	15563	16539
48	23055	24109	26336
54	27859	29079	33398
60	34344	35428	40984

Table A.2. Data from the 2nd experiment

time (h)	1st flask	2nd flask	3rd flask
0	3547	3438	3500
6	4898	3969	4313
12	5820	4695	5016
24	9016	7164	8320
30	11664	9023	10648
36	14078	11000	13492
48	23125	17781	21250
54	27516	22953	27563
60	29597	25798	29194

Table A.3. Data from the 3rd experiment

time (h)	1st flask	2nd flask	3rd flask
0	84259	89352	70988
6	104321	100000	85031
12	127469	120370	98148
24	201698	181327	160494
30	261111	219444	204321
36	335185	289660	265123
48	577469	526235	488735
54	761574	626080	624846
60	962500	855093	795370
78	1300000	1200000	1108333

APPENDIX B: Cell Counting Software

% Matlab Script for Cell Counting

% Path is the location of the folder. User must change the "path" variable

% with respect to the folder he/she uses.

% Sub-folders for the images should be formed as follows:

% C:\ Users\ USER\ Desktop\ images\ c.count\ f.flask \ p.jpg

% where

% c=number of counting done

% f=number of flask that is counted

% p=number of photo taken from each flask

% e.g. C:\ Users\ USER\ Desktop\ images\ 4.count\ 2.flask \ 5.jpg

% indicates the 5th photo taken from 2nd flask

%during the 4th counting process

path = 'C:\ Users\ USER\ Desktop\ images\';

count = '.count\';

flask = '.flask\';

ext1 = '.jpg';

ext2= '.mat';

%number of cells are written to the 3D array solutions

% where

% c_t=total number of counting done

% f_t=total number of flask that is counted

% p_t=total number of photo taken from each flask

% e.g. solutions(2, 4, 5) has the total cell number on 5th photo taken from 2nd flask during the 4th counting process.

solutions = zeros(f_t, c_t, p_t);

for i = 1 : f_t

```
for j = 1 : c_t
    for k = 1 : p_t

%Read the k^th photo taken from i^th flask during the j^th counting
        c_flusk = int2str (i);
        c_say = int2str (j);
        c = int2str (k);
        filename = [path c_say count c_flusk flask c ext1];
        f = imread (filename);
%Extend the intensity range of image
        h= imadjust (f, [0.5 0.75 ], [0 1], 1);
%Apply Gaussian filter to image for noise reduction
        w = fspecial ('gaussian', 4);
        f2 = im2double (h);
        g2 = imfilter (f2, w, 'replicate');
% Shows the improved image on the screen
        imshow (g2);
% User must mark the cells on the figure by right clicking, and
% number will be counted automatically.
% After all cells are marked, the user must click left in order to pass
% the next photo
        button = 1;
        number = 0;
        while (button == 1)
            [x, y, button] = ginput (1);
```

```
                    if (button == 1)
                        number = number + 1;
                    end
                    hold on
                    scatter (x, y, 'x', 'r');
                end
            % After total cell number in each photo is counted,
            % the corresponding number is kept in the 3D array "solutions"
                close all
                solutions (i, j, k) = number;
            end
        end
    end
% After total cell number in all photos are counted, all cell numbers are written
% to the file "total_cell_numbers.mat".
% User can open this file by double clicking on it at the Current Directory
% window on MATLAB.
savefile = [total_cell_numbers ext2];
save (savefile, 'solutions');
```

REFERENCES

1. Cecka, C., A. Davidson, T. Head, D. Mohamed, and L. Robinson, "Modelling Vascular Tumor Growth", Technical Report, Los Alamos National Laboratory, Los Alamos, NM, 2006.

2. Malthus, T. R., *An Essay on the Principle of Population*, J. Johnson, London, 1798.

3. Rudnicki, R., "Models of population dynamics and their applications in genetics", *From Genetics To Mathematics*, 2008.

4. Gompertz, B., "On the Nature of the Function Expressive of the Law of Human Mortality, and on a New Mode of Determining the Value of Life Contingencies", *Phil. Trans. R. Soc. Lond.*, Vol. 115, pp. 513–583, 1825.

5. Verhulst, P. F., "Notice sur la loi que la population suit dans son accroissement", *Corresp. Math. Phys.*, Vol. 10, pp. 113–121, 1838.

6. Allee, W., *Animal Aggregations*, University of Chicago Press, Chicago, 1931.

7. Volterra, V., "Variazioni e fluttuazioni del numero d'individui in specie animali conviventi", *Mem. R. Accad. Naz. dei Lincei*, Vol. 2, pp. 31–113, 1926.

8. Volterra, V., "Fluctuations in the abundance of a species considered mathematically", *Nature*, Vol. 118, pp. 558–560, 1926.

9. Kermack, W. O. and A. G. McKendrick, "A contribution to the mathematical theory of epidemics", *Proc. Roy. Soc.*, Vol. 115, pp. 700–721, 1927.

10. McKendrick, A. G., "Application of mathematics to medical problems", *Proc. Edinb. Math. Soc.*, Vol. 14, pp. 98–130, 1926.

11. Sharpe, F. and A. Lotka, "A problem in age-distributions", *Phil. Mag.*, Vol. 21, pp. 435–438, 1911.

12. Tyson, J. and K. Hannsgen, "Cell growth and division: A deterministic-probabilistic model of the cell cycle", *J. Math. Biol.*, Vol. 23, pp. 231–246, 1986.

13. Tyson, J. and K. Hannsgen, "Asymptotic stability in a generalized probabilistic deterministic model of the cell cycle", *J. Math. Biol.*, Vol. 26, pp. 465–475, 1988.

14. Lasota, A. and M. C. Mackey, "Globally asymptotic properties of proliferating cell populations", *J. Math. Biol.*, Vol. 19, pp. 43–62, 1984.

15. Blythe, R. A. and A. J. McKane, "Stochastic models of evolution in genetics,ecology and linguistics", *J. Stat. Mech.: Theor. Exp.*, 2007, www.iop.org/EJ/abstract/1742-5468/2007/07/P07018.

16. A. Bobrowski, K. P., T. Lipniacki and R. Rudnicki, "Asymptotic behavior of distributions of mRNA and protein levels in a model of stochastic gene expression", *J. Math. Anal. Appl.*, Vol. 333, pp. 753–769, 2007.

17. I, M. G. and G. F. Webb, "A nonlinear structured population model of tumor growth with quiescence", *J. Math. Biol.*, Vol. 28, pp. 671–694, 1990.

18. Nikolai Bessonov, L. P.-M. V. V., Ivan Demin, "A multi-agent model describing self-renewal of differentiation effects on the blood cell population", *Elsevier*, 2008.

19. van der Wath, R. and P. Li, "A Stochastic Multi-agent Model of Stem Cell Proliferation", Umeo, H., S. Morishita, K. Nishinari, T. Komatsuzaki, and S. Bandini (editors), *Cellular Automata*, Vol. 5191 of *Lecture Notes in Computer Science*, pp. 500–505, Springer Berlin / Heidelberg, 2008.

20. Deasy, B., R. Jankowsi, T. Payne, J. Greenberger, and J. Huard, "Modeling stem cell population growth: incorporating parameters for quiescence, differentiation and apoptosis", Vol. 1, pp. 750 – 751, 2002.

21. Jiang, Y., J. Pjesivac-Grbovic, C. Cantrell, and J. Freyer, "A multiscale model for avascular tumor growth", *Biophysical journal*, Vol. 89, No. 6, pp. 3884–3894, 2005.

22. Prince, M., R. Sivanandan, A. Kaczorowski, G. Wolf, M. Kaplan, P. Dalerba, I. Weissman, M. Clarke, and L. Ailles, "Identification of a subpopulation of cells with cancer stem cell properties in head and neck squamous cell carcinoma", *Proceedings of the National Academy of Sciences*, Vol. 104, No. 3, p. 973, 2007.

23. Byrne, H., I. Leeuwen, M. Owen, T. Alarcón, and P. Maini, "Multiscale modelling of solid tumour growth", *Selected Topics in Cancer Modeling*, pp. 1–25, 2008.

24. Britta Bassea, E. S. M. G. C. W. D. J. W., Bruce C. Baguleyb, "Modelling cell population growth with applications to cancer therapy in human tumour cell lines", *Progress in Biophysics and Molecular Biology*, p. 353368, 2004.

25. Pascual, M. and H. Caswell, "From the cell cycle to population cycles in phytoplankton-nutrient interactions", *Ecology*, Vol. 78, No. 3, pp. 897–912, 1997.

26. Ribba, B., T. Colin, and S. Schnell, "A multiscale mathematical model of cancer, and its use in analyzing irradiation therapies", *Theoretical Biology and Medical Modelling*, Vol. 3, No. 1, p. 7, 2006.

27. Gerisch, A. and M. Chaplain, "Mathematical modelling of cancer cell invasion of tissue: local and non-local models and the effect of adhesion", *Journal of theoretical biology*, Vol. 250, No. 4, pp. 684–704, 2008.

28. Armstrong, N., K. Painter, and J. Sherratt, "A continuum approach to modelling cell-cell adhesion", *Journal of theoretical biology*, Vol. 243, No. 1, pp. 98–113, 2006.

29. Abia, L., O. Angulo, J. López-Marcos, and M. López-Marcos, "Numerical schemes for a size-structured cell population model with equal fission", *Mathematical and Computer Modelling*, Vol. 50, No. 5-6, pp. 653–664, 2009.

30. Brikci, F., J. Clairambault, and B. Perthame, "Analysis of a molecular structured

population model with possible polynomial growth for the cell division cycle", *Mathematical and Computer Modelling*, Vol. 47, No. 7-8, pp. 699–713, 2008.

31. Murray, P., C. Edwards, M. Tindall, and P. Maini, "From a discrete to a continuum model of cell dynamics in one dimension", *Physical Review E*, Vol. 80, No. 3, pp. 031912–1, 2009.

32. Foote, C. and E. Edward Chaves, *Cell Division*, available: http://plaza.ufl.edu/alallen/pgl/modules/rio/stingarees/, 2003.

33. Grimes, W. J. and D. Warren, *The Cell Cycle and Mitosis Tutorial*, The Biology Project [Online] Available: http://www.biology.arizona.edu/cell_bio/tutorials/cell_cycle/main.htm, 1997.

34. JR, K., "Enzyme-catalyzed phosphoryl transfer reactions", *Annu. Rev. Biochem*, , No. 49, p. 877919, 1980.

35. Farabee, M. J., *Online Biology Book*, Available: http://www.emc.maricopa.edu/faculty/farabee/BIOBK/BioBookTOC.html, 2001.

36. FWolniak, S. M., *Mitosis*, Lecture Notes, Available: http://www.life.umd.edu/CBMG/faculty/wolniak/wolniakmitosis.html, 2010.

37. Coller, H. A., L. Sang, and J. M. Roberts, "A New Description of Cellular Quiescence", *PLoS Biol*, Vol. 4, No. 3, p. e83, 03 2006, `http://dx.doi.org/10.1371%2Fjournal.pbio.0040083`.

38. Gos, M., J. Miloszewska, P. Swoboda, H. Trembacz, J. Skierski, and P. Janik-Gos, "Cellular Quiescence Induced by Contact Inhibition or Serum Withdrawal in C3H10T1/2 Cells", *Cell Proliferation*, Vol. 38, pp. 107–116, 03 2005.

39. Deasy, B. M., R. J. Jankowski, T. R. Payne, B. Cao, and J. P. Goff, "Modelling Stem Cell Population Growth: Incorporating Terms for Proliferative Heterogene-

ity", *Stem Cells*, Vol. 21, pp. 536–545, 2003.

40. Gutowitz, H., *Cellular Automata: Theory and Experiment*, MIT Press, 1991.

41. Bankhead, A. and R. Heckendorn, "Using evolvable genetic cellular automata to model breast cancer", *Genetic Programming and Evolvable Machines*, Vol. 8, No. 4, pp. 381–393, 2007.

42. Gerlee, P. and A. Anderson, "An evolutionary hybrid cellular automaton model of solid tumour growth", *Journal of theoretical biology*, Vol. 246, No. 4, pp. 583–603, 2007.

43. Alarcon, T., H. Byrne, and P. Maini, "A cellular automaton model for tumour growth in inhomogeneous environment", *Journal of theoretical biology*, Vol. 225, No. 2, pp. 257–274, 2003.

44. Gerlee, P. and A. Anderson, "Stability analysis of a hybrid cellular automaton model of cell colony growth", *Physical Review E*, Vol. 75, No. 5, p. 51911, 2007.

45. Mallet, D. and L. De Pillis, "A cellular automata model of tumor-immune system interactions", *Journal of theoretical biology*, Vol. 239, No. 3, pp. 334–350, 2006.

46. Kari, J., "Theory of cellular automata: A survey", *Theoretical Computer Science*, Vol. 334, No. 1-3, pp. 3–33, 2005.

47. Ren, H., D. Z. Pan, C. J. Alpert, and P. Villarrubia, "Diffusion-based placement migration", *DAC '05: Proceedings of the 42nd annual Design Automation Conference*, pp. 515–520, ACM, New York, NY, USA, 2005.